

Properties of the deconfining phase transition in $SU(N)$ gauge theories

Biagio Lucini^a, Michael Teper^b and Urs Wenger^c

^aInstitute for Theoretical Physics, ETH Zürich,
CH-8093 Zürich, Switzerland

^bTheoretical Physics, University of Oxford,
1 Keble Road, Oxford OX1 3NP, U.K.

^cNIC/DESY Zeuthen, Platanenallee 6, 15738 Zeuthen, Germany

Abstract

We extend our earlier investigation of the finite temperature deconfinement transition in $SU(N)$ gauge theories, with the emphasis on what happens as $N \rightarrow \infty$. We calculate the latent heat, L_h , in the continuum limit, and find the expected behaviour, $L_h \propto N^2$, at large N . We confirm that the phase transition, which is second order for $SU(2)$ and weakly first order for $SU(3)$, becomes robustly first order for $N \geq 4$ and strengthens as N increases. As an aside, we explain why the $SU(2)$ specific heat shows no sign of any peak as T is varied across what is supposedly a second order phase transition. We calculate the effective string tension and electric gluon masses at $T \simeq T_c$ confirming the discontinuous nature of the transition for $N \geq 3$. We explicitly show that the large- N ‘spatial’ string tension does not vary with T for $T \leq T_c$ and that it is discontinuous at $T = T_c$. For $T \geq T_c$ it increases $\propto T^2$ to a good approximation, and the k -string tension ratios closely satisfy Casimir Scaling. Within very small errors, we find a single T_c at which all the k -strings deconfine, i.e. a step-by-step breaking of the relevant centre symmetry does not occur. We calculate the interface tension but are unable to distinguish between the $\propto N$ or $\propto N^2$ variations, each of which can lead to a striking but different $N = \infty$ deconfinement scenario. We remark on the location of the bulk phase transition, which bounds the range of our large- N calculations on the strong coupling side, and within whose hysteresis some of our larger- N calculations are performed.

1 Introduction

In previous papers, [1, 2], we have presented results on some basic properties of the $SU(N)$ deconfining phase transition in $3 + 1$ dimensions, with the emphasis on the order of the transition and the value of the deconfining temperature T_c . In the present paper we shall address a number of more detailed issues such as the physical latent heat, the mass gap and interface tensions. We will also take the opportunity to use some new calculations to improve upon our earlier calculations of $T_c/\sqrt{\sigma}$ where σ is the confining string tension. In a companion paper [3] we have provided a detailed study of the properties of topological fluctuations across the phase transition.

In the next Section we provide a background discussion to motivate the calculations that appear in subsequent sections. We then briefly summarise our (entirely conventional) lattice setup, go on to our improved analysis of $T_c/\sqrt{\sigma}$ and then proceed to our calculation of the physical latent heat and its N -dependence. In the following section we present various mass calculations, both at $T \simeq T_c$ and at higher T . We then address the issue of whether there are multiple deconfining transitions at larger N . We follow this with an estimate of the N -dependence of the confined-deconfined interface tension. We then return to $SU(2)$ to examine more carefully why the usual thermodynamic correlators show no sign of a phase transition in that case. Finally we summarise some properties of the bulk phase transition and how it affects our calculations. In the concluding section we summarise what we have learned in this study, with some comments on large- N Master Fields and Eguchi-Kawai space-time reduction.

2 Deconfinement

In this Section we shall briefly summarise some theoretical expectations for the quantities that we shall calculate later on in this paper.

We begin with a very basic discussion of deconfinement and of the dynamical significance of the order of the transition. We then discuss a new phenomenon that may arise for $N > 3$: deconfinement may occur through several phase transitions rather than just a single one. Although this seems possible on general grounds we shall argue that for dynamical reasons it is very unlikely to occur in the case of $SU(N)$ gauge theories. We then discuss the volume and N dependence of the deconfining transition and how this depends on the N -dependence of the latent heat and of the confining/deconfining interface tension. We describe some of the strikingly simple scenarios that may result at $N = \infty$. We then discuss our expectations for the masses which we calculate below, above and at the phase transition. These include effective string tensions, spatial string tensions and the electric Debye mass. Finally we remind the reader of the fact that not every aspect of the phase transition on our Euclidean space-time volumes is directly reflected in the physics of the hot gauge theory. This will motivate our later investigation of the $SU(2)$ phase transition where, as is well known (at least to practitioners), there is no peak visible in the specific heat despite the apparent second order nature of the transition.

2.1 Introduction

We begin by recalling the following simple argument for deconfinement [4]. Consider two static sources in the fundamental representation that are a distance r apart. Suppose that the theory is linearly confining, so that the flux is restricted to a flux tube of finite width that ends at the two sources. Clearly such a flux tube will be of length $l \geq r$. Consider the case where $l \gg r$. The thermodynamic weight of such a configuration depends on the string energy $E(l) = \sigma l$, where σ is the string tension, as well as on the density of states, i.e. on the number, $n(l)$, of flux tubes of length l with fixed end points:

$$\text{probability} \propto n(l)e^{-\frac{E(l)}{T}} \propto e^{cl}e^{-\frac{\sigma l}{T}}. \quad (1)$$

Here we use the fact that for $l \gg r$ (and ignoring various inessential complications) $n(l) \sim n(l/2)n(l/2)$ so that $n(l) \propto \exp\{cl\}$ up to power corrections. The constant c will depend on the detailed physics of the flux tube. Irrespective of its value, we see from eqn(1) that there is a temperature

$$T = T_c = \frac{\sigma}{c} \quad (2)$$

at which the entropy compensates the Boltzman suppression, so that strings of arbitrary length are produced thermally. Clearly at $T = T_c$ the effective string tension, $\sigma_{eff}(T) = \sigma - cT$, vanishes and the system ceases to be linearly confining.

This simple argument is illuminating in that it makes no reference to any underlying microscopic theory, e.g. to gluons, and shows that any (linearly) confining theory must deconfine at some finite T . Since $\sigma_{eff}(T) \rightarrow 0$ as $T \rightarrow T_c$, the corresponding correlation length diverges and we expect this phase transition to be second order.

Given a phase transition at $T = T_c$ the partition function

$$Z = \sum_{\text{states}} e^{-\frac{E}{T}} \quad (3)$$

should have some singularity there. Since the states contributing to Z are composed of glueballs, it is interesting to ask if there is any argument that Z should be singular at precisely the temperature $T = T_c = \sigma/c$ at which confining strings ‘condense into the vacuum’. We give the following simple argument. A natural model for glueballs is that they are composed of closed loops of confining flux. (See [5] for explicit models of this kind.) For a loop of length l the mass would be $M \simeq \sigma l$. While this dynamics need not be convincing for small l and M (where the size of the state would be comparable to the width of the flux tube) it is hard to imagine excluding its contribution to the very massive glueballs that correspond to large l . Now for large l the number of states should be proportional to the number of different closed loops of length l . This number is clearly $\propto \exp\{cl\}$, with the same exponent c as in eqn(1). Thus Z will be singular at precisely $T = T_c = \sigma/c$ with a Hagedorn-style divergence. (This classical number of states counting should be reliable for the relevant very heavy glueballs on the basis of the standard classical-quantum correspondence for large quantum numbers.) Note that the fact that the lightest glueball is very much heavier than T_c , as are the splittings between the lightest glueballs, should not be regarded as paradoxical (see e.g. [6]); what

matters is the exponential growth of the number of glueball ‘resonances’ and the scale of this growth is, as we have just seen, precisely the same as in the earlier argument for deconfinement through string condensation.

The above discussion has been formulated entirely within the effective low-energy confining theory. This means it does not depend on details, and so possesses an attractive universality, but it also means that it is necessarily incomplete. In particular it ignores the fact that in addition to the energy eigenstates composed of colour singlet glueballs, there are also states composed of gluons where the gluons are densely packed throughout the volume so that they avoid the constraints of confinement (in the same way that dense quark matter avoids these constraints). Neglecting any ambiguity in the separation between these two classes of states, we can write the partition function as

$$Z \simeq \sum_{\text{glueballs}} e^{-\frac{E}{T}} + \sum_{\text{gluons}} e^{-\frac{E}{T}} = e^{-\frac{F_G}{T}} + e^{-\frac{F_g}{T}} \quad (4)$$

where the F_G, F_g are the corresponding free energies. Gluons clearly have an entropy $S_g \propto O(N^2)$ in contrast to the $S_G \propto O(N^0)$ entropy of the colourless glueball states. (This is not quite correct because highly excited glueballs can be composed not only of closed loops of fundamental flux, but also out of closed k -strings with $k \leq N/2$. But this is not important to the present argument.) This means that $F_g = \overline{E}_g - TS_g$ will become equal to $F_G = \overline{E}_G - TS_G$ at some $T = T_c$ and beyond T_c the gluon states will be overwhelmingly more probable – we will be in the ‘gluon plasma’ phase. If this happens at a lower value of T than the ‘string condensation’ temperature discussed earlier, the deconfining phase transition will in fact go directly from a phase with a finite effective string tension to the non-confining ‘gluon plasma’ – and so we would expect it to be first order.

The reason that the confining phase exists at all is that the confining vacuum energy is below that of the ‘perturbative’ vacuum (which one can roughly think of as the vacuum for the states that form the gluon plasma). This difference is often parameterised in terms of the gluon condensate and is usually expected to be $\sim -O(N^2)$. Thus low-lying hadron states are lighter by $O(N^2)V$ than low-lying gluon states. Since at low T energy counts for everything and entropy for nothing, the gluon states are clearly irrelevant there. At large N the value of F_G will be dominated by this vacuum energy at all T , since all other pieces are $O(N^0)$. So it is the competition between this and the $-O(N^2)T$ contribution to the gluon free energy F_g that will determine T_c . Since the vacuum energy density is on the scale of $-O(N^2\sigma^2)$ we would expect

$$\lim_{N \rightarrow \infty} T_c = O(\sqrt{\sigma}) \quad (5)$$

and the fact that this is what one observes [1, 2] may thus be regarded as evidence that the confining vacuum energy density is indeed $-O(N^2)$.

We know that for $SU(N \geq 3)$ gauge theories the phase transition is first order [1, 2] and becomes more strongly so as N increases. This tells us that for these cases deconfinement occurs before the second order string condensation transition has had an opportunity to occur. For $SU(2)$, however, the transition is indeed second order and the effective string tension vanishes as $T \rightarrow T_c^-$. It is therefore possible that here the phase transition proceeds by string

condensation. The same is true of both SU(2) and SU(3) in $D = 2 + 1$. In all these cases the deconfined phase immediately above T_c might exhibit properties very different from those of a gluon plasma and more characteristic of what one would expect in the deconfined phase of a fundamental string theory – an interesting possibility whose investigation lies beyond the scope of the present paper. We note that if we assume the simplest effective string action, the Nambu-Gotto action, and if we assume it to be valid at all scales, then the deconfinement temperature occurs at [7]

$$\frac{T_c}{\sqrt{\sigma}} = \sqrt{\frac{3}{\pi(D-2)}} = \begin{cases} 0.691 & D = 3 + 1 \\ 0.977 & D = 2 + 1 \end{cases} \quad (6)$$

which we can compare to the lattice values [2, 8, 9]:

$$\frac{T_c}{\sqrt{\sigma}} = \begin{cases} 0.709(4) & \text{SU}(2), D = 3 + 1 \\ 1.121(8) & \text{SU}(2), D = 2 + 1 \\ 0.985(12) & \text{SU}(3), D = 2 + 1 . \end{cases} \quad (7)$$

These predicted and lattice values are remarkably close (as has been previously observed [9]), simultaneously suggesting that the Nambu-Gotto action provides a surprisingly accurate representation of the dynamics of the confining flux tube all the way down to scales of $O(T_c)$ and that these phase transitions are indeed driven by ‘string condensation’.

2.2 Multiple transitions?

We have assumed in the above discussion that there is a single deconfinement transition. However this need not be the case. As is well known, deconfinement is associated with the complete spontaneous breaking of a Z_N symmetry, and for $N \geq 4$ this symmetry could be broken in more than one step. In the case of SU(4), for example, one could imagine a breaking $Z_4 \rightarrow Z_2$ at $T = T_c$ followed by a breaking of the remaining Z_2 at $T = T_{c'} > T_c$. Such a pattern of breakings occurs in certain spin models [10] and so is not entirely idle speculation.

Physically such a step-by-step breaking of the Z_N symmetry can be related to the deconfinement of different k -strings at different temperatures $T_c(k)$. Recall (see e.g. [11]) that at low T a source that is like a local clump of k fundamental charges will be joined to a distant conjugate source by a stable flux tube that is called a k -string (for $k \leq N/2$). One can think of a k -string as a bound state of k fundamental strings. The tension of such a string is found to lie somewhere between the Casimir scaling [12] and ‘MQCD’ [13] conjectures [11, 14]:

$$\frac{k(N-k)}{N-1} \leq \frac{\sigma_k}{\sigma} \leq \frac{\sin \frac{k\pi}{N}}{\sin \frac{\pi}{N}}. \quad (8)$$

The two-step deconfinement that we outlined in the previous paragraph would correspond to $k = 2$ charges becoming deconfined at $T = T_c$ while $k = 1$ charges remain confined until a phase transition at a higher temperature $T = T_{c'}$. This can be generalised in an obvious way to larger N and k .

When deconfinement proceeds via string condensation, it is easy to see what is needed for the above scenario to occur. The entropy factor in eqn(1) will in general depend on k , $n_k(l) \propto \exp c_k l$, so that k -strings will condense at

$$T_c(k) = \frac{\sigma_k}{c_k}. \quad (9)$$

If we had no knowledge of the detailed dynamics we could easily imagine that the c_k might be such that a $T_c(k=2) < T_c(k=1)$. (Note that the reverse is not possible because once $k=1$ sources deconfine, all $k > 1$ sources will also deconfine.) However the effective string theory arises from a gauge theory and we will now argue that in a gauge theory this probably cannot occur.

First we note that c_k must contain a factor $1/l_k$ that provides a scale for the l in the exponent. This scale l_k will be given, in the simplest case, by the radius, r_k , of the k -string. This assumes that different flux tubes are geometrically much the same apart from their radii. Now, a flux tube carries non-Abelian electric flux and if we assume that the flux is distributed uniformly across the cross-section of the flux tube, a simple classical calculation would predict

$$\sigma_k \propto \int_0^{r_k} r dr \text{Tr}_k \frac{E E}{r_k^2 r_k^2} \propto \frac{k(N-k)(N+1)}{2N} \times \frac{1}{r_k^2} \quad (10)$$

where we have used the fact that the trace is the quadratic Casimir and we have inserted the value appropriate to a k -source in the totally antisymmetric representation. (This classical calculation is just like the old bag model [15] but without the variational determination of the radius.) Inserting this and $c_k = c_0/r_k$ into eqn(9) we find

$$\frac{T_c(k)}{T_c(k=1)} = \sqrt{\frac{\sigma_k}{\sigma_{k=1}} \frac{k(N-k)}{N-1}} > 1. \quad (11)$$

Although the argument is clearly too simple, the ratio is so much larger than unity that it seems very plausible that fundamental sources must deconfine at the lowest temperature, leading to a simultaneous deconfinement of all other sources.

For $N \geq 3$ and for fundamental sources the phase transition is first order, passing directly to a ‘gluon plasma’ without string condensation. This dynamics will presumably break the centre symmetry completely so that there is a single T_c . The possibility that there might be some earlier second order phase transition corresponding to the condensation of higher k -strings is unlikely given our arguments above coupled to the fact that the first order transition temperature is less than the string condensation temperature of fundamental strings.

Although our conclusion is that there is almost certainly a single deconfinement transition, the possibility that things are otherwise is too interesting to ignore. We therefore perform a numerical investigation in Section 7, although without unearthing any surprises.

2.3 V and N dependence

When the deconfining phase transition is first order, one determines T_c as lying in the range of T where the system undergoes back-and-forth tunnelling between the confined and decon-

finer phases. This tunnelling necessarily proceeds through intermediate field configurations containing two interfaces that divide the periodic spatial volume into roughly two equal parts. Thus, at $T = T_c$ where the two phases have the same free energies, the tunnelling probability will be suppressed as

$$P_{tunnel} \propto \exp\{-2\sigma_{cd}A/T_c\} \quad (12)$$

where σ_{cd} is the surface tension of the interface and A is the (smallest) spatial cross-section, e.g. $A = V^{2/3}$ for a symmetric volume V . So to be able to locate the actual phase transition we need to work on a small enough volume for this tunnelling to be non-negligible. In that case, such back-and-forth tunnelling will occur for a range ΔT of temperatures around T_c for which the difference in the free energies $\Delta F/T$ is $O(1)$. (Once $\Delta F/T \gg 1$ the transition will effectively just go one way.) For T close to T_c we can use the approximation $\Delta F \sim L_h V(1 - T/T_c)$ where L_h is the latent heat (per unit volume) of the transition, and we see that ΔT and hence the uncertainty in locating T_c on the finite volume, is given by

$$\Delta T \propto \frac{T_c^2}{L_h V} \quad (13)$$

Thus we see from eqn(13) that the latent heat determines the uncertainty in determining T_c on a volume V , while eqn(12) tells us that the interface tension determines how large a V one can consider and still see the transition at $T = T_c$. Of course, even if V is so large that no back-and-forth tunnelling can be seen at $T = T_c$, if we move T away from T_c then the growing free energy difference will eventually drive the tunnelling in one direction. The tunnelling will proceed by the formation of a small bubble that grows, improbably, to a certain critical size beyond which the free energy difference between the two phases outweighs the cost of the bubble interface free energy. At this point the bubble will rapidly grow to fill the available volume. (Such a continuous description is appropriate since the lattice Monte Carlo proceeds by changing one link matrix at a time, and so is effectively a continuous deformation of the fields.) It is clear that as the bubble grows, the cost of the bubble will first grow and then decrease. If we estimate the tunnelling probability by the thermodynamic suppression of the most suppressed bubble in this process, we find that for

$$(T - T_c)^2 > c \frac{\sigma_{cd}^3}{L_h^2} T_c \quad (14)$$

(c is some numerical constant) one-way tunnelling will occur however large is the volume. This gives the width of the hysteresis and provides a finite uncertainty on our estimate of T_c if we work on very large volumes. To calculate T_c one therefore works on volumes that are small enough to possess tunnelling right across the transition and one then extrapolates to infinite volume. On the other hand, if we choose to work with V so large that no tunnelling occurs in a (realistic) simulation at $T \simeq T_c$, we will be able to calculate properties of the confining (or deconfined) phase at $T = T_c$ – and in its neighbourhood. We shall make use of this strategy for $N \geq 4$ where the transition is strongly enough first order for this to be practical.

In an earlier paper [2] we performed a calculation of the latent heat at a fixed value of the lattice spacing, $a \simeq 1/5T_c$, and found that

$$L_h \stackrel{N \rightarrow \infty}{\propto} N^2, \quad (15)$$

just as one expects from the usual large- N counting arguments. In the present paper we will calculate the continuum limit of L_h for $N = 4, 6, 8$ and so determine not only the variation with N but also its value in physical units. In [2] we also showed that the interface tension grows with N . In the present paper we attempt to distinguish between $\sigma_{cd} \propto N$ and $\sigma_{cd} \propto N^2$ using a different method, but unfortunately our accuracy will not allow us to answer this question convincingly. (There is a simple theoretical motivation for $\sigma_{cd} \propto N^2$ that has been given in [2].) Each of these two possibilities leads to a particularly simple picture of the phase transition as $N \rightarrow \infty$. We first note from eqn(12) that for either power of N the back-and-forth tunnelling when $T = T_c$ and $\Delta F = 0$ will be exponentially suppressed in N (or in N^2) however small we make V . However we also see from eqn(15) that if $\sigma_{cd} \propto N$ then the width of the hysteresis will be no more than $\Delta T \propto 1/N$. Thus as $N \rightarrow \infty$ on a fixed volume V , however small or large, the phase transition will become completely sharp. If, on the other hand, $\sigma_{cd} \propto N^2$ then this is no longer the case. In this case eqn(14) tells us that on a large volume the hysteresis grows as $\Delta T \propto N$ i.e. becomes infinite at $N = \infty$. In this limit of infinite hysteresis the confined and deconfined phases exist at all T with no tunnelling between them. (If V is smaller, below the critical bubble size, the contribution of the interface tension always dominates as the bubble grows, so this infinite hysteresis scenario would in fact occur on all volumes.) Of course our argument for eqn(14) breaks down once ΔT becomes large, and in any case the string condensation transition will, presumably, intervene somewhere above T_c .

These two ideal scenarios – zero or ‘infinite’ hysteresis on any volume V – provide one motivation for being interested in the value and N -dependence of the interface tension σ_{cd} . Unfortunately the numerical results we present in Section 8 will not be conclusive. All this is also reason to be interested in the latent heat although, since that is a fundamental quantity characterising the phase transition, we would be interested in it in any case. Here our numerical results, in [2] and Section 5 are more precise.

2.4 Masses

The size of the latent heat (rescaled by N^2) tells us how strongly first order the phase transition is. Another measure of this strength is the mass gap in each of the phases as $T \rightarrow T_c$. For a second order transition the mass gap vanishes; for a weakly first order transition it becomes small but non-zero; for a normal first order transition it should be on the order of the typical dynamical length scale of the theory, e.g. T_c or the $T = 0$ string tension. If the mass gap increases with N it provides us with additional evidence that the transition is becoming more strongly first order. We provide some calculations of this mass gap in Section 6.

Since the transition is to do with deconfinement, the natural mass to look at is the effective string tension at finite T , $\sigma_{eff}(T)$. As discussed, for example, in Section 3.1 of [2] this is given

by the mass $m_t(l_t)$ of the lightest flux loop that winds around the timelike torus:

$$\sigma_{eff}(T) = \frac{1}{l_t} m_t(l_t) = T m_t(l_t = \frac{1}{T}). \quad (16)$$

Thus at $T = T_c$ it will be this mass, $m_t(l_t = 1/T_c)$, that will vanish for a second order transition, and should be $\sim T_c$ for a normal first order transition.

Note also that eqn(16) allows us to derive the dependence of $\sigma_{eff}(T)$ on T for low temperatures, $T \sim 0$, in a very simple way. We recall that the leading l_t correction to the linear dependence of $m_t(l_t = 1/T)$ is provided by the universal bosonic string correction, $\pi/3l_t$, so that eqn(16) implies

$$\sigma_{eff}(T) \stackrel{T \rightarrow 0}{=} \sigma - \frac{\pi}{3} T^2 + O(T^4). \quad (17)$$

A parallel argument holds for k -strings and their associated string tensions, at any fixed N . If we take $N \rightarrow \infty$ at fixed k , the k -string becomes an ever more loosely bound state of k fundamental strings and, for reasons discussed in Section 3.1.2 of [14], this implies that the leading correction in eqn(17) will hold in an ever decreasing interval around $T = 0$.

This winding flux loop is the lightest state coupling to timelike Wilson lines (Polyakov loops). In the deconfined phase this operator acquires a non-zero vacuum expectation value. At high T it can be expanded and the first non-trivial term is $\propto Tr\{A_0^2\}$ showing that the strongest coupling of the vacuum subtracted operator will be to two (electric) Debye-screened gluons. To leading order in the 't Hooft coupling, the Debye mass must clearly be $m_D^2 \propto g^2(T)NT^2$ on dimensional grounds, and a one-loop calculation [16] shows that in fact

$$m_t(T) = 2m_D = 2\sqrt{\frac{g^2(T)N}{3}}T. \quad (18)$$

Near $T = T_c$ this perturbative calculation and interpretation is no longer compelling but we shall use the same language for simplicity.

A quite different quantity from the flux loop that winds around the timelike torus is the one that winds around a spatial torus. As $T \rightarrow 0$ this difference disappears of course and either will provide a measure of the $T = 0$ string tension. At high T the mass, $m_s(l_s)$, of this spacelike flux loop and its associated string tension, σ_s , will vary as

$$\sigma_s(l_s; T) = \frac{1}{l_s} m_s(l_s) \propto T^2 \quad (19)$$

on dimensional grounds. The 'spacelike' string tension, σ_s , becomes the string tension of the linearly confining D=2+1 gauge-scalar theory to which the D=3+1 SU(N) gauge theory is dimensionally reduced at high enough T . In principle the spatial string tensions in the confined and deconfined phases at $T \simeq T_c$ could be the same, and this has often been inferred from earlier calculations in SU(3). However when one works at higher N where the phase transition is quite strongly first order, so that the separation into the two phases can be easily made unambiguous, one can show, as we shall in Section 6, that there is in fact a significant discontinuity in σ_s across T_c .

2.5 Thermal average or Euclidean artifact?

In using the Euclidean time framework for calculating thermal averages at a temperature T it is important to be aware that dynamical features of the 4 dimensional Euclidean fields will only be features of the finite temperature field theory if they are encoded as such in the (equal time) thermal averages.

A cautionary example concerns the well-known Z_N spontaneous symmetry breaking of $SU(N)$ gauge theories for $T > T_c$. It is certainly the case that as the Euclidean time extent, l_t , of our 4-volume decreases through the critical value $l_t = 1/T_c$, the 4-dimensional system undergoes a phase transition to one of N degenerate vacua. The timelike Wilson line acquires a value that is proportional to one of the N 'th roots of unity and this serves as an order parameter distinguishing these various phases. There are interfaces between these vacua and these are perturbatively calculable at high enough T [17, 18]. Indeed we note that if we relabel co-ordinates $(x, y, z, t) \rightarrow (t, x, y, z)$ so that the short torus is now in the z -direction and the Euclidean-time torus is now long, so that the theory is effectively at zero temperature, then this phase transition becomes a real finite volume phase transition, obtained by reducing l_z while keeping the other three lengths fixed (and large). All the properties listed above (suitably relabelled) become physically observable. Nonetheless, despite appearances, it is now widely accepted that all this does not mean that the deconfined phase of $SU(N)$ gauge theories possesses such a symmetry breaking with, for example, bubbles of different Z_N vacua in the high- T gluon plasma. At least, no-one has succeeded in showing that such a structure is encoded in an appropriate fashion in equal-time thermal averages. (The timelike Polyakov loop clearly cannot serve such a purpose.)

It is therefore always important to consider if what one is seeing might be a Euclidean artifact rather than a genuine property of the gauge theory at finite T . This applies to the details of the phase transition itself. Of course the first order transitions for $SU(N \geq 3)$ are reflected in discontinuities in thermal averages and there is no ambiguity. However the second order $SU(2)$ transition is more problematic. In particular the diverging correlation length – easily seen in the correlation of timelike Wilson lines – is in practice not visible in equal-time correlators and one finds no growing peak in the specific heat. It is therefore interesting to ask in what way this transition manifests itself in the high- T gauge theory, and this we do in Section 9.

3 The lattice setup

Our Euclidean space-time is discretised to a hypercubic, periodic lattice of size $L_s^3 L_t$ and lattice spacing a , with lengths denoted by L when there is no ambiguity. We assign $SU(N)$ matrices, U_l , to the links l (also denoted by $U_\mu(n)$ for the link emanating in the μ direction from site n). We use the standard plaquette action

$$S = \beta \sum_p \left\{ 1 - \frac{1}{N} \text{ReTr} U_p \right\}, \quad (20)$$

where U_p is the ordered product of the $SU(N)$ matrices around the boundary of the plaquette p . (We shall often use the shorthand $u_p = \text{ReTr}U_p/N$.) S appears in the Euclidean Path Integral as

$$Z = \int \prod_l dU_l e^{-S} \quad (21)$$

and becomes, in the continuum limit, the usual Yang-Mills action with

$$\beta = \frac{2N}{g^2}. \quad (22)$$

Since the theory is asymptotically free, we approach the continuum limit by reducing the bare coupling, $g^2(a) \xrightarrow{a \rightarrow 0} 0$, and so $\beta \rightarrow \infty$. Our simulations in this paper are performed with a combination of heat bath and over-relaxation updates in which we update all the $N(N-1)/2$ $SU(2)$ subgroups of the $SU(N)$ link matrices, as described in [19, 14].

The thermodynamic partition function of the gauge theory at a temperature T is identical to the Euclidean Feynman Path Integral with temporal periodicity of $1/T$. So by calculating appropriate expectation values on an $L_s^3 L_t$ lattice with $L_s \gg L_t$ we are calculating a lattice approximation to the corresponding thermal average at

$$T = \frac{1}{a(\beta)L_t}, \quad (23)$$

which becomes exact when we extrapolate to the continuum limit at fixed T .

When we vary N we expect [20, 21] that we will need to keep constant the 't Hooft coupling, λ ,

$$\lambda \equiv g^2 N \quad (24)$$

to obtain a smooth large- N limit. Non-perturbative calculations for $2 \leq N \leq 5$ have supported this expectation [19]. Using the string tension calculations in our recent paper [14] we can extend this study to $2 \leq N \leq 8$. Following [19] we define a (lattice improved) 't Hooft coupling on the scale a by

$$\lambda_I(a) = g_I(a)^2 N = \frac{2N^2}{\beta \langle u_p \rangle} \quad (25)$$

and plot in Fig.1 the result. We observe very nice evidence that the running 't Hooft coupling approaches a limiting N -independent function of the length scale $l = a\sqrt{\sigma}$ as $N \rightarrow \infty$, and that it does so very rapidly, once we are away from the coarsest values of a that are close to the bulk transition/cross-over (see Section 10).

Finally two comments for the general reader.

Our Monte Carlo generates a sequence of fields by changing the value of one link matrix at a time, with the local action density controlling the size of the change. Thus the Monte Carlo proceeds by what is essentially a local deformation of the fields and so it mimics features of a real phase transition in a statistical mechanics system. That is to say, a first order transition can be described as a continuous tunnelling process, in terms of growing bubbles of one phase

within another phase, and if at $T = T_c$ that probability is low enough then we will observe a hysteresis effect.

Our second comment is that the deconfining phase transition occurs only on physical length scales. Thus in lattice units the latent heat will be $a^4 L_h \propto a^4 \xrightarrow{a \rightarrow 0} 0$ and the mass gap at the transition will also satisfy $am_g \xrightarrow{a \rightarrow 0} 0$. So from the point of view of the lattice, the transition is very weakly first order and becomes second order as $a \rightarrow 0$. This is however an illusion, merely reflecting the fact that the continuum limit is a second order transition of the lattice theory. When we express the mass gap and latent heat in physical units, e.g. as L_h/T_c^4 and m_g/T_c , it becomes clear that the transition is robustly first order for $N \geq 4$.

4 The deconfining temperature

Since presenting our results on $T_c/\sqrt{\sigma}$ in [2] we have significantly improved our SU(8) calculations. We now have a greater range of volumes at $L_t = 5$ and this allows us to obtain a more reliable estimate of the coefficient h of the leading $1/V$ correction to β_c :

$$\beta_c(V) \stackrel{V \rightarrow \infty}{\cong} \beta_c(\infty) - h \frac{L_t^3}{L_s^3}. \quad (26)$$

We also have better calculations of the SU(8) lattice string tensions [14] and this allows us to perform a more accurate continuum extrapolation of $T_c/\sqrt{\sigma}$.

We recall [2] that our strategy is to use the value of h calculated at $a = 1/5T_c$ to perform $V \rightarrow \infty$ extrapolations at the smaller values of a at which we usually have performed calculations on only one volume. In [2] we did not attempt to compute the a -dependence of h and we simply doubled the statistical error on h in the hope that this would encompass any variation of h with $a(\beta)$. However the form of this a dependence of h is known [2]

$$h(a) \stackrel{a \rightarrow 0}{\cong} \frac{h_0}{\frac{d}{d\beta} \ln a(\beta = \beta_c)} + O(a^2) \quad (27)$$

and so we can use the values of $d \ln a / d\beta$ that we calculate later on in this paper to rescale h at the β values of interest. We shall do this not just for $N = 8$, but for $N = 4, 6$ as well. We then increase the error on h by 15% in order to cover the remaining $O(a^2)$ corrections which, given what we observe with other dimensionless quantities, we expect to be small.

In Tables 1 – 3 we list our calculated values of the critical β , obtained by extrapolating to $V = \infty$ using eqns(26,27) with the values of h as shown. We calculate the string tension at each β using the values in [14] and this provides us with the listed values of $T_c/\sqrt{\sigma}$. Comparing with Table 5 of [2] we see that the SU(4) and SU(6) values have changed very little, while the SU(8) values, where we employ better calculations of σ , have changed more substantially.

We extrapolate to the continuum limit using an $a^2\sigma$ correction, as described in [2], and list the resulting continuum values of $T_c/\sqrt{\sigma}$ in Table 4. For completeness we have included the SU(2) and SU(3) values although their analysis is unchanged from [2]. We note that the fits all have an acceptable χ^2 per degree of freedom except for SU(4) where the fit is very poor.

This promises to create a problem for any statistical analysis that involves the SU(4) value, as for example in the extrapolation to $N = \infty$ to which we now turn.

In Fig.2 we plot our continuum values of $T_c/\sqrt{\sigma}$ against $1/N^2$. The usual large- N counting tells us that the leading large- N correction should be $O(1/N^2)$, and this corresponds to a straight line on this plot. While it is clear that our results do fall approximately onto a straight line, the best fit χ^2 is in fact very poor. It is reasonable to suppose that this is due to our SU(4) value being off perhaps by several standard deviations. To try and deal with this we rescale the errors on the SU(4) lattice calculations by almost a factor of two, so that the continuum extrapolation has a χ^2 per degree of freedom of unity. This increases the error on the continuum extrapolation to the value shown in square brackets in Table 4. Performing a fit with this modified SU(4) error, we obtain

$$\frac{T_c}{\sqrt{\sigma}} = 0.5970(38) + \frac{0.449(29)}{N^2} \quad (28)$$

with an acceptable χ^2 per degree of freedom of about unity. This fit is plotted in Fig.2. As we have noted before [1, 2] it is remarkable and perhaps puzzling that the leading correction suffices all the way down to SU(2) despite the fact that the transition changes from first to second order between $N = 3$ and $N = 2$.

In performing our large- N extrapolation we assume a conventional $O(1/N^2)$ correction. Since this expectation is based on diagrams (albeit to all orders) while $T_c/\sqrt{\sigma}$ is a non-perturbative quantity, it is interesting to see whether our results are accurate enough to constrain the power of the leading correction. We therefore perform fits to a $1/N^\alpha$ correction. We find that the χ^2 per degree of freedom of the best fit is

$$\frac{\chi^2}{n_{df}} = \begin{cases} 3.5 & : \alpha = 1 \\ 0.8 & : \alpha = 2 \\ 3.1 & : \alpha = 3 \end{cases} \quad (29)$$

which provides some evidence that the leading correction is indeed $O(1/N^2)$.

5 Latent heat

5.1 Background

The free energy, F , and the free energy per unit volume, f , are defined to be

$$Z \equiv \sum_{states} e^{-\frac{E}{T}} = e^{-\frac{F}{T}} = e^{-\frac{fV}{T}} \quad (30)$$

where V is the spatial volume and Z is the standard finite temperature partition function. The internal energy density, ϵ , is the average energy per unit volume

$$\epsilon \equiv \frac{\overline{E}}{V} = \frac{T^2}{V} \frac{\partial}{\partial T} \ln Z. \quad (31)$$

Suppose we are on a $L_s^3 L_t$ lattice that remains fixed in lattice units. The Euclidean Feynman Path integral provides a definition of a thermodynamic partition function of the lattice system at $T = 1/aL_t$ which will tend to the desired continuum partition function as we reduce a (as long as the spatial volume is sufficiently large). a and hence T are varied by varying β , so eqn(31) becomes

$$\epsilon = \frac{T^2}{V} \frac{\partial \beta}{\partial T} \frac{\partial}{\partial \beta} \ln Z = \frac{T^2}{V} \left\{ -L_t a^2 \frac{\partial \beta}{\partial a} \right\} \left\{ 6L_s^3 L_t \langle u_p \rangle \right\} = -6 \frac{\langle u_p \rangle}{a^4} a \frac{\partial \beta}{\partial a} \quad (32)$$

where $\langle u_p \rangle$ is the average plaquette. We thus see that the latent heat in units of T_c is given by

$$\frac{L_h}{T_c^4} \equiv \frac{\Delta \epsilon}{T_c^4} = -L_t^4 a \frac{\partial \beta}{\partial a} 6 \Delta \langle u_p \rangle. \quad (33)$$

Note that if we wished to calculate the internal energy or the free energy, we would need to be concerned about regularising it, for example by subtracting from $\langle u_p \rangle$ in eqn(32) the value of the plaquette at some reference value of T (but at the same value of a). Since we are only interested in the difference in internal energies, such issues need not concern us here.

The finite T phase transition is clearly also a phase transition of a statistical system in 4 space dimensions whose classical partition function is our Euclidean Feynman path integral. In this reinterpretation, β is the inverse temperature and the action S is the energy. In this case the latent heat is simply the jump in the action i.e. it is just what we find in eqn(33) but without the factor of $a \partial \beta / \partial a$. This latter factor is, however, crucial if we want to obtain an estimate of the real deconfining latent heat of the gauge theory in 3 space dimensions.

We can calculate $a \partial \beta / \partial a$ using

$$a \frac{\partial \beta}{\partial a} = a \mu \frac{\partial \beta}{\partial (a \mu)} \quad (34)$$

where μ is some physical quantity with dimensions of mass, e.g. $\mu = \sqrt{\sigma}$ or $\mu = T_c$. Such different choices will differ by $O(a^2)$ lattice corrections in $\Delta \epsilon / T_c^4$. We shall choose to use $\mu = \sqrt{\sigma}$. To obtain the value of $\partial(a\sqrt{\sigma})/\partial\beta$ at the values of β that correspond to $T = T_c$ for various values of L_t we interpolate between our calculated values of $a\sqrt{\sigma}$ (as listed in Tables 5-9 of [14]) using a fitting function

$$a\sqrt{\sigma(\beta)} = c_0 \exp \left\{ -\frac{12\pi^2}{11} \frac{(\beta - \beta_0)}{N^2} + c_1 x + c_2 x^2 + c_3 x^3 \right\} \quad ; \quad x \equiv N^2 \left(\frac{1}{\beta} - \frac{1}{\beta_0} \right). \quad (35)$$

The value of β_0 is chosen to coincide with one of the calculations near the middle of the interesting range of β . (Given that we fit c_0 , this is not an extra parameter.) Where we can obtain a good fit without the $O(x^3)$ term we do so. Note that although the fitting function is designed so that it automatically tends to one-loop scaling at large enough β , the particular form of the fit does not really matter as long as we intend to use it to interpolate rather than to extrapolate in β . (Including a $\ln \beta$ term corresponding to 2-loop scaling does not improve the fits and does not even appear to improve the rate at which scaling is approached when the fits are extrapolated to larger β .) In Table 5 we list the values of the parameters of the best fit for each N together with the range of β interpolated (and the χ^2 per degree of freedom of the best fit).

5.2 Results

In [2] we calculated the value of $\Delta\langle u_p \rangle$ from the $V \rightarrow \infty$ limit of the specific heat peak. (Note that in [2] we referred to this as L_h , and the latent heat was defined as the jump in the average ‘energy’ per plaquette of the four dimensional lattice system. This differs from the physical latent heat of the three dimensional thermal gauge theory, as discussed above.) This calculation requires a detailed finite volume study, which we have only carried out at $a \simeq 1/5T_c$, with the results shown in Table 6, and so it is only at this fixed lattice spacing that we have been able to compare latent heats for different N . What we would now like to obtain is the comparison in the continuum limit, and for that we need a different technique.

We begin by observing that on our very largest lattice volumes at $a \simeq 1/5T_c$ there is no tunnelling for $N \geq 4$ at $T \simeq T_c$ in our simulations. We can therefore produce ensembles of lattice fields that are entirely confining or deconfining by obtaining the starting lattice field from $T \rightarrow T_c^-$ and $T \rightarrow T_c^+$ respectively (and subsequently thermalising at $T = T_c$). From these two ensembles we can calculate $\langle u_p \rangle_c$ and $\langle u_p \rangle_d$, respectively, and hence $\Delta\langle u_p \rangle$. The values of the latter are listed in the $L_t = 5$ rows of Table 7. They are all compatible with the values obtained from the specific heat extrapolation, as listed in Table 6, reinforcing our confidence in both methods.

We can extend this method to smaller volumes where the tunnelling is present but is relatively rare. We can use the mean Polyakov loop as an order parameter to categorise subsequences in the Monte Carlo generated sequence of lattice fields as being confined, deconfined or (much more rarely) tunnelling. There is clearly some ambiguity in this separation, but this ambiguity disappears as the tunnelling becomes less frequent. We try to incorporate this ambiguity into the error estimate by using various different cuts on the order parameter and by averaging the order parameter over subsequences of lattice fields of different length. However once the spatial volume becomes sufficiently small in physical units – as measured by L_s/L_t – all these remedies become inadequate and our values will be increasingly unreliable. A test of this method for the case of SU(4) can be found in Fig.5 of [1] where the $L = 32$ lattice has no tunnelling and provides the benchmark for the comparison. We observe that the error becomes rapidly larger as we decrease V , as it should, but that the value of $\Delta\langle u_p \rangle$ remains consistent with the $V \rightarrow \infty$ value, even on the smallest volumes where some separation between phases is apparent. This reassures us that this method can be used at smaller values of a where we do not have calculations on volumes that are very large in physical units.

Our results are listed in Table 7. For $N \geq 4$ we have three values of L_t . Since our calculations are at a fixed temperature, $T \simeq T_c$, we have $a \propto 1/L_t$ and this will allow us to perform a continuum extrapolation. At each N and L_t we have used only the largest lattices. We show the value of β at which $\Delta\langle u_p \rangle$ is calculated. In fact around each of these values of β there are usually two or three nearby values which exhibit tunnelling and are useful. We transport these values to the indicated value, varying a^4 using the listed values of $\partial\beta/\partial \ln a$. We then transport from these reference values of β to the values of $\beta_c(V = \infty; L_t)$ listed in Tables 1-3 and using eqn(33) we obtain the latent heat at $T = T_c$ in physical units, as shown. We now discuss these results.

Our best values of L_h , in the sense of possessing the smallest statistical and systematic

errors, are those for $L_t = 5$. In Fig.3 we plot these latent heats against $1/N^2$ and show a fit of the form

$$\frac{1}{T_c} \left\{ \frac{L_h}{N^2} \right\}^{\frac{1}{4}} = c_0 + \frac{c_1}{N^2}. \quad (36)$$

This form is expected because the average energy of the gluon plasma should be $O(N^2)$ and the leading large- N correction should be $O(1/N^2)$. We see that L_h/N^2 does indeed appear to go to a finite limit and that the SU(3) value is well below the fit, in line with the usual belief that it is weakly first order. We note that L_h/N^2 increases to an $N = \infty$ limit that is $O(1)$ in units of T_c . That is to say, the transition is robustly first-order in that limit.

In Fig.4 we plot the dimensionless ratio $L_h^{\frac{1}{4}}/T_c$ against $a^2 T_c^2$. For the plaquette action the leading lattice correction is known to be $O(a^2)$ so we expect to be able to extrapolate to the continuum limit using

$$\frac{L_h^{\frac{1}{4}}(a)}{T_c(a)} = \frac{L_h^{\frac{1}{4}}(a=0)}{T_c(a=0)} + ca^2 T_c^2(a). \quad (37)$$

Unfortunately it is clear that such straight-line fits will be very poor and indeed they lead to $\chi^2/n_{df} \simeq 3, 9, 11$ for $N = 4, 6, 8$ respectively, which is unacceptable. All the plots show the similar feature that the $L_t = 5$ value is much too high to lie on the fit. Although in some cases L_s/L_t is smaller for $L_t = 6$ than for $L_t = 8$, in other cases it is larger, so we do not attribute the problem to large finite volume corrections afflicting all the $L_t = 6$ calculations. We therefore take this to be a real effect rather than a manifestation of some unexpectedly large systematic error. That means that we must extrapolate using just the two values, at $L_t = 6$ and at $L_t = 8$. This means we have no evidence that including just the $O(a^2)$ correction is sufficient. Nonetheless, it is plausible to assume that it is since for other quantities, such as glueball masses, the deconfining temperature, etc., we know that it is in this range of a . Making this assumption we obtain the continuum values listed in Table 8, using the extrapolations shown in Fig.4.

We can now take these continuum values of $L_h^{\frac{1}{4}}/T_c$ and see whether they determine the $N = \infty$ value. We find that they are indeed well fit by the expected functional form

$$\frac{L_h^{\frac{1}{4}}}{N^{\frac{1}{2}} T_c} = 0.766(40) - \frac{0.34(1.60)}{N^2} \quad : \quad \chi^2/n_{df} = 0.3, \quad (38)$$

although the errors are rather large because of the fact that we could not use our most accurate data, which was at $L_t = 5$.

As we shall discuss in Section 10, the value of β corresponding to $a = 1/5T_c$ is very close to the bulk transition. This is a rapid crossover for $N = 4$, and becomes a strong first order transition for $N \geq 6$. Indeed, for $N = 8$, $a = 1/5T_c$ is very close to the lower β edge of the bulk hysteresis curve. At this first order bulk transition the jump in the plaquette, $\Delta\langle u_p \rangle$, is about 50 times larger than it is for the deconfining transition on the $L_t = 5$ lattice system. It is therefore plausible that the whole effective potential is becoming deformed at this value of a and that this is causing the anomalously large value for the latent heat at $L_t = 5$. The fact that the effect is larger for $N = 6, 8$ than for $N = 4$, where the transition is only a

crossover, supports this hypothesis. This transition can be naturally regarded as a finite N manifestation of the D=1+1 Gross-Witten transition [22, 23] and the plaquette is the natural order parameter. It is therefore perhaps plausible that it should be the average plaquette that is most sensitive to the nearby presence of the bulk phase.

6 Masses

At $T = T_c$ we can perform calculations separately in the confined and deconfined phases by working with volumes large enough for there to be no sign of any tunnelling (or attempted tunnelling). We have performed such calculations on $32^3 5$, $16^3 5$ and $12^3 5$ lattices for SU(4), SU(6) and SU(8) respectively. In SU(3) we use a $64^3 5$ lattice, on which there is tunnelling, but it is very rare and we can work with long subsequences of field configurations that are in a single phase. (The reason that we are able to work on smaller spatial volumes, $V = l_s^3$, as N increases is because in the tunnelling probability, $\propto \exp\{-2\sigma_{cd}l_s^2/T\}$, the interface tension, σ_{cd} , increases with N – as discussed in Section 8.) Although the calculations in this Section are performed at a fixed value of the lattice spacing, this value is small enough that the results should be representative of what one would obtain in the continuum limit.

6.1 Mass gap at $T = T_c$

We calculate the lightest mass that couples to the Polyakov loop which winds around the time-torus. We do this for different k -loops (see Section 2.2) at each value of N and we present the masses for the confined and deconfined phases in Tables 9 and 10 respectively. (In the deconfined phase we use the vacuum subtracted loop.)

We observe that in the confined phase the higher k loops are more massive, just as they are at $T = 0$. If we take the mass of the SU(8) loop in the confined phase, and apply the leading string correction (*a priori* inadequate for such a short string) so as to extract a string tension $\sigma = m/l_t + \pi/3l_t^2$, we obtain, for SU(8), a value, $a\sqrt{\sigma} \simeq 0.314(3)$ that is quite close to the $T = 0$ value $a\sqrt{\sigma} \simeq 0.346$ [14]. This suggests that this first order transition is quite strong. If we express the loop mass in the natural units of T_c and plot it, in Fig.5, against $1/N^2$ we see that this mass gap tends to a finite $N = \infty$ limit, albeit with a large $O(1/N^2)$ correction. Indeed we see that for SU(3) the correlation length, $\xi_t = 1/m_t$, is quite large indicating a transition that is quite weakly first order.

The $k = 2$ mass gap in Fig.5 also appears to tend to a finite $N = \infty$ limit. Although we have used a leading $O(1/N^2)$ correction, this is not guaranteed to be correct for $k > 1$ strings. The alternative is an $O(1/N)$ correction which arises in, for example, the Casimir Scaling conjecture [12]. It is interesting to note that the string tension ratio

$$\frac{\sigma_{eff}(k=2)}{\sigma_{eff}(k=1)} = \frac{m_t(k=2)}{m_t(k=1)} \xrightarrow{N \rightarrow \infty} \begin{cases} 1.91 \pm 0.13 & \delta\sigma_{k=2} = O(1/N^2) \\ 2.36 \pm 0.21 & \delta\sigma_{k=2} = O(1/N) \end{cases} \quad (39)$$

is compatible with the value of 2 that one expects from factorisation in the $N = \infty$ limit (even at finite T) for both forms of the correction.

In the deconfined phase all the k -loops couple to the same object (the centre symmetry is spontaneously broken) and, as we see in Table 10, their masses are the same. (It is interesting to note that the operator with the largest k appears to have the best overlap.) Writing this mass as twice the Debye mass, we plot its value against $1/N^2$ in Fig.6. Once again we see a finite large- N limit with a large finite- N correction that leads to a small SU(3) mass, confirming its weakly first order character.

It is of course quite possible that some of our calculated masses suffer significant finite volume corrections. To partially address this question we show in Table 11 the masses one gets in SU(4) on smaller lattices at the same value of a . The smaller the lattice the greater the tunnelling and the more difficult it is to distinguish the two phases, hence the increasing errors. To partially control this we also show some calculations performed at slightly different values of β where there is very little tunnelling. The conclusion of this comparison is that the confined $k = 1$ mass has at most modest corrections but that they may be more substantial for the $k = 2$ mass. In the deconfined phase, any finite V correction to the $L_s \geq 20$ calculations look small. Since finite V corrections are likely to be functions of the lattice size in units of the mass, the above suggests that our SU(6) and SU(8) lattices are large enough for the confined $k = 1$ masses and probably large enough for the deconfined masses, but that the $k > 1$ confined masses may well suffer substantial corrections. (See also [24].)

6.2 Debye mass at $\mathbf{T} > \mathbf{T}_c$

We see from eqn(18) that at leading order in $g^2(T)N$ the Debye electric screening mass m_D is independent of N and grows linearly in T up to the weakly varying coupling factor.

We extract this mass from correlations of the vacuum-subtracted timelike Polyakov loop on $L_s = 8$ lattices with $L_t = 2, 3, 4$ at a value of β where $L_t = 5$ corresponds to $T = T_c$ and list the results in Table 12. Thus our lattice calculations cover the range $1.25 \leq T/T_c \leq 2.5$. In the case of SU(8) the tunnelling on an $8^3 5$ lattice is sufficiently well-defined that we are able to separate fields in the confined and deconfined phase and so calculate m_D down to $T = T_c$. For $T = T_c$ we also have calculations on the larger volumes listed in Table 10. We see that at $T = T_c$, where the masses are smallest, the finite V shift is at the level of $\sim 20\%$. At the highest T , where the masses are largest, we have also performed calculations on $6^3 2$ lattices, for SU(4) and SU(8), and there is no finite V shift visible within quite small errors.

In Fig.7 we plot $m_t = 2m_D$ against T/T_c for both SU(8) and SU(3). We observe that for $T \geq 5T_c/3$ the mass is independent of N and appears to increase $\propto T$. There are only small deviations from this behaviour at $T = 5T_c/4$ and it is only at $T \simeq T_c$ that we see any large deviation.

Thus the asymptotic $T \rightarrow \infty$ behaviour sets in very close to T_c , especially at larger N . This is remarkable since for $T \sim T_c$ the coupling will surely not be small. Indeed, if we apply eqn(18) to our calculated values, we find

$$\frac{g^2(T \simeq 1.25T_c)N}{4\pi} \simeq 0.43. \quad (40)$$

Such a substantial coupling also means that the lowest order calculation is probably unreliable

(as may be the interpretation of m_t as $2m_D$). Indeed eqn(18) would predict that the approach to the linear behaviour at high T should be from above, since $g^2(T)$ decreases with increasing T , whereas what we observe in Fig.7 is that it does so from below.

6.3 Spatial string tensions at all T

The expectation values of large spatial Wilson loops are known to decay exponentially with their area at all T and the coefficient of the area is the ‘spatial string tension’. At high T this corresponds to the string tension of the dimensionally reduced $D = 2 + 1$ $SU(N)$ gauge-Higgs theory. It also corresponds to the string tension in a $L_s^2 L_t$ spatial volume at a temperature $aT = 1/L_s$, for sources separated along one of the long directions. (This follows from a trivial relabelling of the Euclidean co-ordinates.)

The spatial string tension, $\sigma_s(T)$, can be obtained from the correlation of Polyakov loops that wind around a spatial torus. From this we obtain the ‘mass’, m_s , of the lightest flux loop that winds around that torus and applying the usual string correction, which should be adequate since L_s is large, we obtain the spatial string tension:

$$\frac{1}{L_s} am_s(L_s; T) = a^2 \sigma_s(T) - \frac{\pi D_\perp}{6} \frac{1}{L_s^2}. \quad (41)$$

Here D_\perp is the number of dimensions transverse to the Wilson loop. For $D=3+1$ and low T we have $D_\perp = D - 2 = 2$ and we would expect this to remain the case for any T in the confining phase. It is less clear what one should use in the deconfined phase: at very large T one presumably has $D_\perp = 1$. Since eqn(19) tells us that $\sigma_s(T) \propto T^2$, this correction will be $O(1/T^2)$ and so unimportant at high T if L_s is kept fixed.

Below T_c $\sigma_s(T)$ is more-or-less constant and above T_c it grows with T . Is the change smooth or discontinuous? Given that the transition is first-order a discontinuity would be natural but the existing folklore, based on $SU(3)$ calculations, is that it is continuous. To address this question we show in Table 13 the values of am_s as obtained on sequences of 12^{35} lattices at $T = T_c$ in $SU(8)$, that are entirely in confined and deconfined phases respectively. (These volumes are large enough to suppress any sign of tunnelling.) What we actually show in the Table are effective masses obtained from local cosh fits to the correlation function. They are labelled by the distance n_t at which they are calculated. Although the errors become large for $n_t \geq 3$ (particularly in the confined phase) it is quite clear that there is a discontinuity in the value of m_s as we cross from the confined to the deconfined phase. (The string operators we use have excellent overlaps onto the lightest string states, and we expect [14] the $n_t = 2$ effective mass to provide an excellent approximation to the true mass.) Since the transition is strongly first order for $SU(8)$, perhaps the real surprise is that this jump (decrease) in the spatial string tension is only about 15%.

From Table 13 we estimate am_s in the confined phase to be $am_s = 1.377(40)$. Using eqn(41) with $D_\perp = 2$ we then obtain $a\sqrt{\sigma_s}(T = T_c) = 0.349(5)$. We can compare this to the ‘ $T = 0$ ’ value by interpolating to $\beta = 43.965$ the values in Table 9 of [14] giving $a\sqrt{\sigma_s}(T = 0) = 0.346(2)$. Thus we see that to a good approximation the spatial string tension does not change at all when T increases from 0 to T_c – at least for large enough N .

We have also calculated am_s on the $L_s = 8$ and $L_s = 6$ lattices that were used in Section 6.2 to calculate the T -dependence of the electric gluon mass in the deconfined phase. The extracted loop masses are listed in Table 14. In Fig.8 we plot the $k = 1$ spatial loop mass against $(T/T_c)^2$, since that is the expected behaviour at high T (see eqn(19)). We plot the best linear fits to the data and we clearly observe good evidence for the early onset of the quadratic behaviour. We note that the $T = 0$ intercept corresponds to relative corrections that are $O(1/T^2)$, and which include the string correction. We note some variation of the slope with N , but this is close to what we have observed [2] in the variation of $T_c/\sqrt{\sigma}$ with N and so it is presumably an $O(1/N^2)$ correction.

In Fig.9 we plot the ratios of the k -loop masses to the fundamental ($k = 1$) loop masses. At higher T , where string corrections become negligible, this just becomes the ratio of the corresponding spatial k -string tensions. For comparison we show the predictions of the Casimir scaling conjecture [12] in eqn(8). (This also arises naturally in a model where the high- T plasma contains a gas of adjoint magnetic pseudo-particles [25].) It is clear from Fig.9 that we have quite good agreement with this conjecture. By contrast, the trigonometric ‘MQCD’ conjecture in eqn(8) is strongly disfavoured. The inclusion of a string correction strengthens this conclusion.

7 $\mathbf{T}_c(\mathbf{k})$

We pointed out in Section 2.2 that deconfinement may proceed in several discrete steps, if the relevant Z_N centre symmetry breaks through a sequence of subgroups. In that case different k -string operators will acquire non-zero expectation values at the corresponding temperatures, $T_c(k)$. As we remarked in Section 2.2 one expects, on general grounds, that $T_c(k) \leq T_c(k = 1)$. Thus the temperature we have identified as T_c using the $k = 1$ Polyakov loop as the order parameter, will be the highest of these temperatures. If, then, we calculate the masses of the various k -strings in the confined phase at $T = T_c(k = 1)$, any such expectation values will become manifest, and we will have direct evidence for the existence of such multiple phase transitions.

We have performed such mass calculations for many of the values of N , lattice sizes and β values discussed in Section 6. In Table 9 we summarised some of our ‘cleanest’ results. These calculations were performed without any vacuum subtraction so that a non-zero vacuum expectation value would manifest itself in a (nearly) vanishing mass gap. It is clear that none of the masses are near zero, demonstrating that in all these case the k -string operators have not developed non-zero expectation values for $T < T_c(k = 1)$. This provides our first, quite convincing evidence that deconfinement proceeds through a single phase transition.

Of course the reason the mass calculations in Table 9 are ‘clean’ is that the spatial volumes used are large enough for the confined-deconfined tunnelling to be negligible. One might therefore worry that even if there was an earlier phase transition, the corresponding tunnelling would be improbable. This is clearly not going to be the case unless the $T_c(k)$ are sufficiently close, since otherwise the free energy difference between the relevant phases will promote the tunnelling probability at $T_c(k = 1)$. Nonetheless this uncertainty suggests that we should also

look at smaller volumes where there is significant tunnelling. We have indeed done so and find no suggestion for non-zero expectation values for any $k > 1$ string operators. Such a study does however suffer from some small ambiguity to do with separating the confined and deconfined phases on smaller volumes.

As an explicit illustration, we consider $SU(4)$. We take the largest lattice, 20^{35} , on which we see any tunnelling (within our statistics) and a value of T slightly below T_c ; roughly $T \simeq 0.996T_c$. In Fig.10 we plot a histogram of the values taken by $|\bar{l}_{k=1}|$, the modulus of the Polyakov loop averaged over a single lattice field configuration. We see the very large peak at low $|\bar{l}|$ corresponding to the confined phase (l is complex hence the suppression at $l = 0$) and a small peak at larger $|\bar{l}|$ corresponding to fields in the deconfined phase. If there was a separate $k = 2$ transition then we would expect that some of the fields in the low $|\bar{l}_{k=1}|$ peak in Fig.10 would be confined for $k = 2$ strings and some would be deconfined. To test whether this is so we have taken separately all the fields with $|\bar{l}_{k=1}| \leq 0.05$ and $|\bar{l}_{k=1}| > 0.05$ (i.e. mid-way between the confined and deconfined peaks) and for each of these two ensembles we plot separately the distribution of $|\bar{l}_{k=2}|$ (in the totally antisymmetric representation). These are plotted in Fig.11 and we see that there is no evidence at all for a $k = 2$ deconfined phase for which $k = 1$ strings are still confined. We infer that there is a single deconfining transition at any N .

8 Interface tensions

We saw in Section 2.3 that at $T = T_c$ the interface tension, σ_{cd} , determines the rate of tunnelling between the confined and deconfined phases through eqn(12). In this Section we shall use the observed rate of tunnelling to estimate the N -dependence of σ_{cd} , borrowing standard methods that have been used in earlier work [26] in the case of $SU(3)$. (For a different approach, which appeared as this paper was being written, see [27].) We shall start by formulating in more detail the expression for tunnelling, with the focus on making explicit all the important N -dependence.

We use the average Polyakov loop on each lattice field, \bar{l} , as our order parameter. (In practice we will use its modulus, which leads to some minor changes as described in [26].) Let $i = c, d$ label the confined and deconfined phases and let $P_i(\bar{l})$ be the normalised probability distribution. If ξ_i is the length scale on which the fluctuations of Polyakov loops decorrelate, and if V is large enough, then we can expect that making the usual assumption of a single-scale Gaussian distribution

$$P_i(\bar{l}) = c_i e^{-\frac{(\bar{l}-\bar{l}_i)^2}{d_i^2}} \quad (42)$$

where

$$\frac{1}{d_i^2} \propto N^2 \frac{V}{\xi_i^3} \quad ; \quad c_i \propto \frac{1}{d_i} \quad (43)$$

is a harmless approximation for our purposes. The factor of N^2 in eqn(43) follows from the usual large- N factorisation arguments for gauge invariant operators, which imply that $\langle \bar{l}^2 \rangle = \langle \bar{l} \rangle^2 (1 + O(1/N^2))$ in both phases.

At $T = T_c$ we have tunnelling and both Gaussian peaks are present. The probability that a value of \bar{l} mid-way between the peaks comes from one of these Gaussians is $\propto \exp\{-b_i N^2 V\}$, where the b_i are some constants, and this is much less than the tunnelling probability, $\propto \exp\{-2\sigma_{cd} A/T\}$, for large enough V and/or N . So in the latter limit, on an $L_s^3 L_t$ lattice, the observed probability of such a value of \bar{l} should reflect the tunnelling probability

$$p_t \propto e^{-2\frac{a^2\sigma_{cd}L_s^2}{T}} = e^{-2a^3\sigma_{cd}L_s^2L_t} \quad (44)$$

in lattice units.

Let us assume that we have defined T_c on a finite volume as the temperature at which the probability of the confined phase equals that of the deconfined phase. (The maximum of the specific heat or of the loop susceptibility will correspond to this definition at large V .) We see from the above that if we consider the overall probability distribution for \bar{l} then the value at the minimum p_{min} , between the two Gaussian peaks, is related to the value at one of these peaks, p_{max} , by

$$\frac{p_{min}}{p_{max}} \propto \frac{L_s^2 e^{-2a^3\sigma_{cd}L_s^2L_t}}{\sqrt{N^2V}} = \frac{L_s^{\frac{1}{2}}}{N} e^{-2a^3\sigma_{cd}L_s^2L_t}. \quad (45)$$

The factor of L_s^2 comes from translations of the two walls (and being careful with the way this affects the measure). The fact that there are N deconfined phases in the Euclidean system does not alter this result. Note that we have neglected the contribution from the interiors of the domain walls and various factors that have non-zero large- N limits.

Apart from the obvious caveats, an additional uncertainty in the above analysis is that it ignores the contribution of tunnellings between the N different deconfined phases. If we label the deconfined vacuum by k , corresponding to the k 'th element of Z_N , then one can see that a tunnelling between the k and k' vacua will pass through fields with

$$|\bar{l}| \simeq |l_d| \cdot \left| \cos\left\{\pi \frac{k - k'}{N}\right\} \right|. \quad (46)$$

For $k - k' \sim O(N/2)$ the value of $|\bar{l}|$ will be partway between $|l_c|$ and $|l_d|$, i.e. precisely where we have applied eqn(45). Since we expect (at least at high T where it is calculable [17]) that $\sigma_{kk'} \sim O(N^2)$ when $k - k' \sim O(N/2)$, such tunnellings are strongly suppressed, and will only be important for $N, V \rightarrow \infty$ if $\sigma_{cd} \sim O(N^2)$ so that the deconfining tunnellings are similarly suppressed. In principle one can identify and exclude these deconfined-deconfined tunnellings. In practice this requires large enough V for the transitions to be very well separated. This represents a potentially significant systematic error.

As an aside, we remark that the above problem only arises because we have chosen to use \bar{l} as our order parameter. We could use the average plaquette instead since that also takes different values in the confined and deconfined phases. However because its value is the same in all N deconfined vacua, tunnellings between the latter will not populate the range of plaquette values that signal tunnelling between confined and deconfined phases. The reason we do not analyse the plaquette probability distributions is that the separation between the Gaussian peaks is essentially non-existent for our range of V and N .

Since our calculations are at $T \simeq T_c$ it is customary to define the dimensionless surface tension

$$\hat{\sigma}_{cd} \equiv \frac{\sigma_{cd}}{T_c^3} \quad (47)$$

in which case we see from eqn(45) that

$$\hat{\sigma}_{cd} = -\frac{L_t^2}{2L_s^2} \ln \frac{p_{min}}{p_{max}} + \frac{L_t^2}{2L_s^2} \left\{ \frac{1}{2} \ln L_s - \ln N + c \right\} \quad (48)$$

where c is a constant which may contain large $O(1/N^2)$ corrections. Capillary waves along the interface [28] produce a constant that can be absorbed into the c in eqn(48). (The next correction [28] is $O(1/L_s^2)$ and we shall ignore it here.) We now apply the above formalism, and calculate $\hat{\sigma}_{cd}$ from our calculated Polyakov loop probability distributions.

In our calculation we choose T_c as the temperature at which the peak heights of the confined and deconfined Polyakov loop probability distributions are equal. This differs slightly from our above discussion but, since both peaks shrink with N and V in the same way, this does not affect the argument in a material way. Defining

$$\hat{\Sigma}_{cd} \equiv -\frac{L_t^2}{2L_s^2} \ln \frac{p_{min}}{p_{max}} + \frac{L_t^2}{4L_s^2} \ln L_s \quad (49)$$

we see from eqn(48) that

$$\begin{aligned} \hat{\Sigma}_{cd} &= \hat{\sigma}_{cd} - \frac{L_t^2}{2L_s^2} \left\{ c - \ln N \right\} + \dots \\ &\xrightarrow[\frac{L_s \rightarrow 0}{L_t \rightarrow 0}]{} \hat{\sigma}_{cd}. \end{aligned} \quad (50)$$

In Fig.12 we plot our calculated values of $\hat{\Sigma}_{cd}$ against $(L_t/L_s)^2$ and show the best fits obtained by including the leading large- V correction shown in eqn(50). We note that the slope of the best fit decreases with increasing N whereas from eqn(50) one would expect the opposite. It is clear that higher order corrections in N or V must be important here. For example, we find that the two Gaussian distributions are not well separated for most of our volumes. Thus there must be some doubt about the reliability of our large- V extrapolations.

Ignoring this uncertainty, we extract the interface tensions from the large- V extrapolations in Fig.12 and list them in Table 15. Plotting them against N in Fig.13 we observe a very strong increase with N . The fact that σ_{cd} increases by a factor of ~ 30 when we go from SU(3) to SU(8) implies, using eqn(44), that we must decrease L_s by a factor ~ 5.5 if we want to maintain a comparable tunnelling rate when we go from $N = 3$ to $N = 8$.

To test the functional form of the increase of σ_{cd} with N , we show in Fig.13 the best fits corresponding to both linear

$$\frac{\sigma_{cd}}{T_c^3} = 0.118(3)N - 0.333(9) \quad ; \quad \chi^2/n_{df} = 6.5 \quad (51)$$

and quadratic variations

$$\frac{\sigma_{cd}}{T_c^3} = 0.0138(3)N^2 - 0.104(3) \quad ; \quad \chi^2/n_{df} = 2.7. \quad (52)$$

While a cursory glance at Fig.13 might have suggested that a linear behaviour looks better, we see that this is not supported by the statistical analysis which strongly prefers $\sigma_{cd} \propto N^2$. However the χ^2 is driven by the very accurate smaller- N values, which might be sub-asymptotic. So it is clear that more accurate calculations with a better control of the systematic errors are needed, particularly for $N \geq 8$, if we are to be able to answer this question.

9 SU(2)

The SU(2) gauge theory is linearly confining at low T and deconfined at high T . Therefore there will be a phase transition at some $T = T_c$. If the phase transition were first order then, in the $V = \infty$ thermodynamic limit, $\partial \ln Z / \partial \beta$ would be discontinuous at $T = T_c$. This is the case, as we have seen, for $N \geq 3$. In SU(2), however, it is well known that there is no observed discontinuity, and that instead the effective string tension appears to vanish smoothly as $T \rightarrow T_c^-$. The corresponding correlation length diverges as $T \rightarrow T_c^-$ and the transition is thus taken to be second order.

In Fig.14 we provide an example of how the correlation length varies with β and the spatial volume on a set of $L^3 5$ lattices for which $V = \infty$ deconfinement occurs at $\beta_c = 2.3714(6)$ (see Table 4 of [2]). What is actually shown here is $\xi_t = 1/am_t$ where m_t is the mass of the lightest flux loop that winds around the time-torus, and which is related to $\sigma_{eff}(T)$ by eqn(16) when $V \rightarrow \infty$. We see how on a fixed volume near T_c the value of ξ_t is constrained by the spatial size, but that it is consistent with diverging at T_c as we take $V \rightarrow \infty$. This is to be contrasted with the values of am_t at $T = T_c$ for $N \geq 3$ that are listed in Table 9 (for the same value of a in units of T_c).

The usual way to identify a first or second order transition at $\beta = \beta_c$ is to calculate the specific heat $C(\beta)$

$$\frac{1}{\beta^2} C(\beta) = \frac{1}{V} \frac{\partial^2 \ln Z(\beta)}{\partial \beta^2}. \quad (53)$$

If V is finite but large, then $C(\beta)$ should have a peak at some $\beta = \beta_c(V) \xrightarrow{V \rightarrow \infty} \beta_c$ and this peak should diverge as

$$C(\beta_c(V)) \propto V^\alpha \quad (54)$$

where $\alpha = 1$ for a first order transition and $\alpha < 1$ for a second order transition. The behaviour for a first order transition follows trivially from the discontinuity in the action, when one notes that C is proportional to the integrated connected plaquette correlation function

$$C(\beta) \propto \frac{1}{V} \langle \sum_p u_p \sum_{p'} u_{p'} \rangle - \langle \sum_p u_p \rangle^2 \propto \sum_p \langle (u_p - \bar{u})(u_{p_0} - \bar{u}) \rangle. \quad (55)$$

Of course it will only be seen if the Monte Carlo calculation is long enough to sample both phases. For a second order transition the divergence of C arises because of the vanishing mass, which implies a divergence in the integrated correlator in eqn(55). For the first order transition, for $N \geq 3$, a growing specific heat peak is precisely what we see. However for the SU(2) transition $C(\beta)$ not only does not grow with V in the neighbourhood of β_c , but shows no peak at all; despite the fact that, as we see in Fig.14, there is a rapidly growing correlation length for these volumes. This is the implicit reason why earlier studies have not used $C(\beta)$ to study the SU(2) transition, but have rather used the Polyakov loop susceptibility, which shows the expected diverging behaviour.

We are already familiar with one example of a striking phenomenon in the high T Euclidean system which is visible in Polyakov loops but which is not directly reflected in the real thermal properties of the gauge theory: the Z_N symmetry breaking and vacuum degeneracy discussed in Section 2.5. Here we have a diverging correlation length which has only been visible in Polyakov loops. Is it possible that this divergence is also not reflected in the thermal properties of the gauge theory, so that the phase transition is not second but higher order? This may seem very unlikely but provides us with a motivation for understanding better what is going on.

The vanishing of the mass of the timelike flux loop at β_c implies, from eqn(16), the vanishing of the effective string tension, $\sigma_{eff}(T)$, at $T = T_c = 1/a(\beta_c)L_t$. When we calculate the overlap of our (unsmeared) Polyakov loop onto this lightest flux loop, at say $\beta = 2.3725 \simeq \beta_c$, we see that it remains very large, ~ 0.95 , on all our volumes. This implies that the effective potential between static sources will show a linear behaviour $V(r) \simeq \sigma_{eff}(T)r$ from some relatively short distance, and that the potential will flatten from this distance onwards as $T \rightarrow T_c$. Thus the vanishing of the SU(2) effective string tension at the transition is a robust, highly visible feature of the thermal gauge theory.

Nonetheless this is a property of the gauge theory probed with static fundamental sources, and is not related in an obvious way to the vanishing in the pure gauge theory of a screening length which couples to the plaquette. Indeed we know that in the confining phase a non-contractible winding flux loop must have an exactly zero overlap on to a contractible Wilson loop such as the plaquette, and so cannot contribute directly to $C(\beta)$. But this is not the end of the story. Scattering states composed of two such (mutually conjugate) flux loops will have energies all the way down to zero at T_c and these can have non-zero overlaps onto the plaquette. We now estimate this overlap.

Consider a 20^{35} lattice at $\beta_c = 2.3675$, which is very close to β_c . We consider operators composed of $\vec{p} = 0$ sums of spatial (magnetic) and timelike (electric) plaquettes and also an operator that is composed of a product of two $\vec{p} = 0$ Polyakov loops. (Since we reserve the label t for the short torus, we take correlations in the z -direction and the momentum \vec{p} is defined in the 3-space orthogonal to the latter.) Looking at the effective mass plot of the latter it is clear that at this a this operator has a very good overlap onto the state composed of two of the lightest $\vec{p} = 0$ timelike flux loops. We will therefore make the approximation that this operator is in fact the wavefunctional for this two loop state, $|ll\rangle$. We label the latter operator by ϕ_{ll} , and the plaquette sums by u_s, u_t respectively. Then the normalised

cross-correlations give us the matrix element which determines the desired overlap

$$\frac{\langle vac|u_a\phi_U|vac\rangle}{\langle vac|u_a u_a|vac\rangle^{\frac{1}{2}}\langle vac|\phi_U\phi_U|vac\rangle^{\frac{1}{2}}} \simeq \frac{\langle vac|u_a|ll\rangle}{\langle vac|u_a u_a|vac\rangle^{\frac{1}{2}}} \simeq \begin{cases} 0.027(3) & : a = s \\ 0.042(3) & : a = t. \end{cases} \quad (56)$$

This is very small, and one naturally wonders if this smallness does not indicate that the overlap actually vanishes either as one approaches $V = \infty$ or as one approaches $\beta = \beta_c$. This we shall now show is not the case. We have performed calculations on 14^{35} and 12^{35} lattices which show that the overlap in eqn(56) is volume independent, within errors. We have also performed calculations at $\beta = 2.3600$ where $T - T_c$ is about 3 times larger than in the above example, and again we find that the overlap is unchanged. We thus conclude that at the lattice spacing $a \simeq 1/5T_c$ there is in fact a non-zero overlap between the plaquette and the double flux loop whose mass, we recall, vanishes as $V \rightarrow \infty$ and $T \rightarrow T_c$. That is to say, the thermal average of a plaquette-plaquette correlator must, at large enough separations, display the contribution of this diverging correlation length, and so the deconfining transition in the SU(2) thermal gauge theory is indeed a conventional second order one.

In the normalised $\vec{p} = 0$ plaquette-plaquette correlator, the contribution of the double flux loop will be

$$\frac{C_{uu}(n_z)}{C_{uu}(0)} = \frac{|\langle vac|u_a|ll\rangle|^2}{\langle vac|u_a u_a|vac\rangle} e^{-2am_t n_z} + \dots \quad (57)$$

(ignoring periodicity). We can use this to estimate how large we have to make L_s for the diverging correlation length to start making a visible contribution. First we note that we can replace $\sum_p u_p$ in eqn(55) by the sum over z of the $\vec{p} = 0$ sums of plaquettes. And we can make a crude estimate for $am_t(L_s)$ using Fig.14. Using the latter and the overlaps in eqn(56), we can easily see, via a very approximate calculation, that for the term in eqn(57) to contribute about half of the specific heat at $\beta = \beta_c$, we need to have a lattice with $L_s \sim 2000$. It is now clear why even on our ‘very large’ 40^{35} lattices we saw no sign of a growing specific heat peak!

The above calculations have been for a specific small range of a close to $a = 1/5T_c$. As $a \rightarrow 0$ all physical states decouple from the plaquette, since wavelengths on physical scales contribute only $\sim a^4 \Lambda_{QCD}$ of its value. So in the continuum one would want to use a suitably regularised form of the action when calculating the specific heat. Since we have no reason to expect any pathology as $a \rightarrow 0$ we have not attempted a detailed study at smaller a . We have however performed some calculations at $a = 1/8T_c$ which confirm that the overlap, as defined in eqn(56), remains non-zero, and that it is smaller, roughly as one would expect.

Finally we comment that the above near-decoupling will obviously also occur for $N > 2$ where the transition is first order. This means that the specific heat will give a clear, precocious signal for the developing two peak structure in the plaquette distribution, unobscured by an additional term coming from an increasing correlation length (albeit increasing only to some finite value). This is to be contrasted with the Polyakov loop susceptibility. This effect is strongest for the weakly first order transition in SU(3) – compare Fig.5 and Fig.3 in [2].

10 The bulk phase transition

It is well known that SU(2) and SU(3) lattice gauge theories with the plaquette action exhibit a rapid crossover between the strong and weak coupling regions. This crossover becomes more pronounced for SU(4) [29] and, as we have found in the present work, transforms into a weakly first order transition for SU(5) and becomes robustly first order for SU($N \geq 6$). The strong coupling bulk phase is believed to contain Z_N vortices and monopoles which disorder Wilson loops down to the ultraviolet length scale, so that the string tension in lattice units is $a^2\sigma \sim O(1)$. On the weak coupling side, the physics in the ultraviolet is determined by asymptotic freedom and so $a^2\sigma \sim O(a^2) \ll 1$. Only calculations on the weak coupling side are useful for the continuum extrapolation.

The $N \rightarrow \infty$ limit has been studied within the twisted Eguchi-Kawai formalism, and the critical inverse bare 't Hooft coupling is [30]

$$\lambda_b^{-1}(N = \infty) = \lim_{N \rightarrow \infty} \frac{\beta_b}{2N^2} = 0.3596(2). \quad (58)$$

In Table 16 we list the values of β_b that we have obtained for $5 \leq N \leq 12$ during the course of our calculations. For $N = 5$ we can estimate β_b directly but for $N \geq 6$ the interface tension becomes large enough that all we see is a hysteresis effect. Once the interface tension is large the size of the hysteresis varies weakly with both the volume size, as we see in Table 16, and also with the length of Monte Carlo run at each value of β (within practical limits). This leads to a large uncertainty in β_b , which can be eliminated by adding a suitable function of the order parameter to the action, as in [30]. However our purpose here is not to study the bulk transition *per se* but rather to determine its influence, if any, on our calculations of T_c . Nonetheless we note that our results for $N \geq 6$ are consistent with eqn(58) together with a modest $O(1/N^2)$ correction. (Note that this will not be the same $O(1/N^2)$ correction as determined in [30] since the Eguchi-Kawai equivalence only exists at the leading planar level.)

We compare the values of β_b in Table 16 to the values of β_c in Tables 1-3. We note that for SU(6) the deconfining transitions for $L_t \geq 5$ are safely beyond the bulk transition. Interpolating to SU(5) we would expect the $L_t = 5$ deconfining transition to be at $\beta_c(L_t = 5) \simeq 16.87$, which is again well beyond β_b . For SU(8) on the other hand, the hysteresis has widened and now encompasses both $\beta_c(L_t = 5)$ and $\beta_c(L_t = 6)$. These calculations of β_c have been performed by working on the weak coupling branch of the hysteresis curve and clearly we need to know if this introduces a bias.

A useful order parameter for the bulk transition is the average plaquette \bar{u}_p . For larger N its discontinuity is $\Delta\bar{u}_p \sim 0.13$. Thus, in contrast to the deconfining transition, where the discontinuity is only $O(a^4)$, here it is $O(1)$ and so even partial tunnellings are easily visible on single lattice fields. We have examined the plaquette distributions at $\beta \simeq \beta_c(L_t = 5)$ and we find no trace of even a partial attempt at tunnelling. It is clear that the barrier between the bulk and weak coupling phases is so large that the deconfining phase transition in the weak coupling phase at $a \simeq 1/5T_c$ is largely unaffected by the fact that it occurs in only a local rather than in the absolute minimum of the effective potential – except perhaps for some minor distortion of the potential that we have earlier hypothesised might be the reason for

the unexpectedly large lattice spacing corrections to the latent heat at this a .

11 Conclusions

In this paper we studied various properties of $SU(N)$ gauge theories at and around the deconfining phase transition. We checked that there is indeed only one transition, i.e. that the centre symmetry is not broken in steps, with each step corresponding to the condensation of an appropriate k -string. We showed that the transition is robustly first order at large N with a latent heat $L_h \propto N^2$ as expected, and an interface tension σ_{cd} that grows with N , although our calculations were unable to determine whether this growth is $\propto N$ or $\propto N^2$. In the former case the transition would become a real phase transition even on a small volume as $N \rightarrow \infty$ (which is possible because the number of degrees of freedom per unit volume diverges in that limit). In the latter case one expects a growing hysteresis, even on small volumes. If this hysteresis is large enough one might encounter the ‘Hagedorn’ string condensation transition along the confining branch, above T_c .

We calculated the spatial string tension and showed that at larger N its value in the confining phase appears to be entirely independent of T . However, when we compare the spatial string tensions in the two phases at $T = T_c$ it is clear that there is a significant discontinuity. This is easy to see for larger N because the transition is robustly first order and the growing interface tension ensures that even on moderately large lattices there is no tunnelling, or even attempted tunnelling. So one can study the properties of the two phases separately at $T = T_c$. For example, on a $12^3 5$ lattice for $SU(8)$. By contrast, in the well-studied case of $SU(3)$, even on a $64^3 5$ lattices we still observe tunnelling. Thus such a discontinuity has not been observed in $SU(3)$ although it undoubtedly exists there as well.

At higher T we have seen that the spatial string tension grows $\propto T^2$ and that it does so essentially from $T = T_c$ for larger N . The spatial k -string tensions are consistent with Casimir Scaling. For high T the Debye mass grows $\propto T$ as expected, although there are large deviations near T_c . This is not surprising because the leading-order theoretical expression, $m_D^2 \propto g^2(T)T^2$ contains an additional ‘logarithmic’ dependence on T in the coupling.

We also showed why the $SU(2)$ transition has no peak in the specific heat, let alone one that grows with V , although there is a diverging correlation length. We explicitly showed that this correlation length will eventually appear as a visible screening length in thermal averages, so that the transition is a bona fide second order one. For larger N we discussed the bulk transition, in the shadow of whose hysteresis we have performed some of our deconfinement studies.

The main motivation for studying $SU(N)$ gauge theories at large N is the hope that $SU(3)$ might be ‘close’ to this limit and the gauge theory is expected to be much simpler at $N = \infty$ than at $N = 3$. The former has been largely confirmed by recent lattice calculations [19, 14, 2]. Signs of the latter are found throughout our calculations in this paper; for example the reduction in finite volume effects at the deconfinement transition, which naturally points [2] to a form of Eguchi-Kawai space-time reduction [31]. On the other hand, while the suppression of ‘small’ fluctuations as $N \rightarrow \infty$ does indeed lead to the simple idea of a Master Field [32],

what we have also seen is that there is actually a plethora of Master Fields – confining, deconfining, bulk, one for each of the N degenerate phases obtained if a spatial torus is reduced below a critical size, not to mention the N θ -vacua branches [33] and conjectured non-analyticities in scale size [34]. All this [23] serves to emphasise how much there is still to be understood about the physics of this theory.

Acknowledgements

Our lattice calculations were carried out on the JIF/PPARC funded Astrophysics Beowulf cluster in Oxford Physics, on PPARC and EPSRC funded Alpha Compaq workstations in Oxford Theoretical Physics, on a desktop funded by All Souls College, and on the APE in Swansea Physics funded by PPARC under grant PPA/G/S/1999/00026. During much of this research, UW was supported by a PPARC SPG fellowship, and BL by a EU Marie Skłodowska-Curie postdoctoral fellowship. MT would like to thank the KITP for its hospitality while this paper was being written up, and would like to thank participants at the ‘QCD and String Theory’ Workshop at the KITP, as well as at the ‘Large N ’ and ‘QCD and Strings’ Workshops at the ECT, Trento, for useful and interesting discussions.

References

- [1] B. Lucini, M. Teper and U. Wenger, Phys. Lett. B545 (2002) 197 (hep-lat/0206029).
- [2] B. Lucini, M. Teper and U. Wenger, JHEP 0401 (2004) 061 (hep-lat/0307017).
- [3] B. Lucini, M. Teper and U. Wenger, hep-lat/0401028.
- [4] A. Polyakov, Phys. Lett. B72 (1978) 477.
- [5] N. Isgur and J. Paton, Phys. Rev. D31 (1985) 2910.
T. Moretto and M. Teper, hep-lat/9312035.
R. Johnson and M. Teper, Phys. Rev. D66 (2002) 036006 (hep-ph/0012287).
- [6] N. Ishii and H. Suganuma, hep-ph/0210158.
- [7] J. Arvis, Phys. Lett. 127B (1983) 106.
M. Luscher and P. Weisz, JHEP 0407 (2004) 014 (hep-th/0406205).
- [8] M. Teper, Phys. Lett. B313 (1993) 417 and unpublished.
- [9] J. Engels, F. Karsch, E. Laermann, C. Legeland, M. Lutgemeier, B. Petersson and T. Scheideler, Nucl. Phys. Proc. Suppl. 53 (1997) 420 (hep-lat/9608099).
- [10] C. Korthals Altes, private communication.

- [11] B. Lucini and M. Teper, Phys. Lett. B501 (2001) 128 (hep-lat/0012025); Phys. Rev. D64 (2001) 105019 (hep-lat/0107007).
- [12] J. Ambjorn, P. Olesen and C. Peterson, Nucl. Phys. B240 (1984) 189, 533; B244 (1984) 262; Phys. Lett. B142 (1984) 410.
- [13] A. Hanany, M. Strassler and A. Zaffaroni, Nucl. Phys. B513 (1998) 87 (hep-th/9707244).
M. Strassler, Nucl. Phys. Proc. Suppl. 73 (1999) 120 (hep-lat/9810059).
M. Strassler, Prog. Theor. Phys. Suppl. 131 (1998) 439 (hep-lat/9803009).
- [14] B. Lucini, M. Teper and U. Wenger, JHEP 0406 (2004) 012 (hep-lat/0404008).
- [15] T. H. Hansson, Phys. Lett. B166 (1986) 343.
K. Johnson and C. B. Thorn, Phys. Rev. D13 (1976) 1934.
- [16] D. Gross, R. Pisarski and L. Yaffe, Rev. Mod. Phys. 53 (1981) 43.
- [17] P. Giovannangeli and C. P. Korthals Altes, Nucl. Phys. B608 (2001) 203 (hep-ph/0102022); hep-ph/0412322.
- [18] C. Korthals Altes, A. Michels, M. Stephanov and M. Teper, Phys. Rev. D55 (1997) 1047 (hep-lat/9606021).
- [19] B. Lucini and M. Teper, JHEP 0106 (2001) 050 (hep-lat/0103027).
- [20] G. 't Hooft, Nucl. Phys. B72 (1974) 461.
E. Witten, Nucl. Phys. B160 (1979) 57.
S. Coleman, 1979 Erice Lectures.
A. Manohar, 1997 Les Houches Lectures, hep-ph/9802419.
S.R. Das, Rev. Mod. Phys. 59(1987)235.
Y. Makeenko, hep-th/0001047.
- [21] G. 't Hooft, in *Large N QCD* (Ed. R.F. Lebed, World Scientific 2002) (hep-th/0204069); hep-th/0408183.
- [22] D. Gross and E. Witten, Phys. Rev. D21 (1980) 446.
- [23] M. Teper, Talk at 'Large N QCD', ECT, Trento July 2004 (hep-th/0412005).
- [24] H. Meyer and M. Teper, hep-lat/0411039.
- [25] C. Korthals Altes, hep-ph/0406138; hep-ph/0408301.
- [26] Y. Iwasaki, K. Kanaya, L. Karkainen, K. Rummukainen and T. Yoshie, Phys. Rev. D49 (1994) 3540 (hep-lat/9309003).
- [27] Ph. de Forcrand, B. Lucini and M. Vettorazzo, hep-lat/0409148 and in preparation.

- [28] M. Caselle, R. Fiori, F. Gliozzi, M. Hasenbusch, K. Pinn and S. Vinti, Nucl. Phys. B432 (1994) 590 (hep-lat/9407002).
- [29] B. Lucini and M. Teper, JHEP 0106 (2001) 050 (hep-lat/0103027).
- [30] M. Campostrini, Nucl. Phys. Proc. Suppl. 73 (1999) 724 (hep-lat/9809072).
- [31] T. Eguchi and H. Kawai, Phys. Rev. Lett. 48 (1982) 1063.
A. Gonzales-Arroyo and M. Okawa, Phys. Lett. 120B (1983) 174.
- [32] E. Witten, in: “Recent Developments in Gauge Theories”, Ed. G. 't Hooft et al. (Plenum Press, 1980).
- [33] E. Witten, Phys. Rev. Lett. 81 (1998) 2862 (hep-th/9807109).
G. Gabadadze and M. Shifman, Int. J. Mod. Phys. A17 (2002) 3689 (hep-ph/0206123).
A. Armoni and M. Shifman, Nucl. Phys. B 664 (2003) 233 (hep-th/0304127).
- [34] R. Narayanan and H. Neuberger, Talks at ‘Large N QCD’, ECT, Trento July 2004 (hep-lat/0501031).

SU(4)				
L_t	L_s	h	$\beta_c(V = \infty)$	$T_c/\sqrt{\sigma}$
5	12-20	0.090(17)	10.63727(53)	0.6148(13)
6	16	0.100(22)	10.7898(16)	0.6166(24)
8	24	0.123(27)	11.0880(22)	0.6310(30)

Table 1: Critical values of β calculated on $L_s^3 L_t$ lattices and extrapolated to $V = \infty$ using eqn(26) and the values of h shown. The corresponding values of $T_c/\sqrt{\sigma}$ are shown.

SU(6)				
L_t	L_s	h	$\beta_c(V = \infty)$	$T_c/\sqrt{\sigma}$
5	8-14	0.112(19)	24.5139(24)	0.5894(36)
6	16	0.128(29)	24.8467(30)	0.5956(29)
8	16	0.168(39)	25.4782(64)	0.6024(29)

Table 2: Critical values of β calculated on $L_s^3 L_t$ lattices and extrapolated to $V = \infty$ using eqn(26) and the values of h shown. The corresponding values of $T_c/\sqrt{\sigma}$ are shown.

SU(8)				
L_t	L_s	h	$\beta_c(V = \infty)$	$T_c/\sqrt{\sigma}$
5	8,10	0.134(73)	43.982(14)	0.5819(41)
6	8	0.155(84)	44.535(37)	0.5850(70)
8	10,12	0.218(123)	45.654(32)	0.5888(69)

Table 3: Critical values of β calculated on $L_s^3 L_t$ lattices and extrapolated to $V = \infty$ using eqn(26) and the values of h shown. The corresponding values of $T_c/\sqrt{\sigma}$ are shown.

SU(N) : continuum		
N	$T_c/\sqrt{\sigma}$	χ^2/n_{df}
2	0.7091(36)	0.28
3	0.6462(30)	0.05
4	0.6344(42)[(81)]	3.7[1.0]
6	0.6101(51)	0.02
8	0.5928(107)	0.003

Table 4: $T_c/\sqrt{\sigma}$ extrapolated to the continuum limit for various SU(N) gauge theories, with the χ^2 per degree of freedom of the best fits. The SU(2) and SU(3) values are taken from [2].

N	$\beta \geq$	$\beta \leq$	β_0	c_0	c_1	c_2	c_3	χ^2/n_{df}
2	2.1768	2.5115	2.3726	0.2877	0.9195	-3.2961	–	0.55
3	5.6925	6.3380	5.8945	0.2607	2.6312	12.2494	24.0	0.54
3	5.6925	6.3380	5.8945	0.2610	2.7271	10.6846	–	1.1
4	10.637	11.400	10.789	0.2702	3.5393	18.7900	–	0.9
6	24.500	25.452	24.670	0.3082	4.9649	34.5288	–	0.5
8	43.85	45.700	44.350	0.3022	5.0812	42.0732	–	1.2

Table 5: Fit parameters to the string tension as a function of β using the interpolation function in eqn(35).

N	L_t	$L_s \in$	$\Delta\langle u_p \rangle$
3	5	20-40	0.00084(2)
4	5	14-20	0.00198(5)
6	5	8-14	0.00238(6)
8	5	8-10	0.00251(34)

Table 6: The jump in the average plaquette, $\Delta\langle u_p \rangle$, between the confined and deconfined phases at $\beta_c(a = 1/5T_c)$, as obtained from a $V \rightarrow \infty$ extrapolation of the specific heat peak from the range of lattice sizes shown.

L_h at $a = 1/L_t T_c$						
N	L_t	L_s	β	$\Delta\langle u_p \rangle$	$d \ln a / d\beta$	L_h / T_c^4
3	5	64	5.799	0.00078(3)	-2.070(9)	1.413(55)
4	5	32	10.635	0.00187(4)	-1.2878(90)	5.39(13)
	6	16	10.780	0.00064(5)	-1.1666(80)	4.06(34)
	8	24	11.085	0.000165(20)	-0.9400(90)	4.30(53)
6	5	16	24.515	0.00248(3)	-0.6347(120)	14.69(35)
	6	16	24.845	0.00084(2)	-0.5472(80)	11.90(35)
	8	16	25.46	0.000202(7)	-0.4012(76)	12.00(49)
8	5	12	43.965	0.00261(4)	-0.3717(54)	25.67(65)
	6	8	44.45	0.00075(5)	-0.3240(26)	16.0(1.4)
	8	12	45.50	0.000195(10)	-0.2304(48)	17.8(1.1)

Table 7: The jump in the average plaquette, $\Delta\langle u_p \rangle$, and the latent heat, L_h , at $T = T_c$, for the gauge groups and parameters shown.

L_h : continuum		
N	$L_t \in$	$L_h^{\frac{1}{4}}/T_c$
4	6,8	1.47(10)
6	6,8	1.87(5)
8	6,8	2.12(9)

Table 8: The latent heat in physical units after a continuum extrapolation from the $L_t = 6, 8$ values.

am_k at $a \simeq 1/5T_c$: confined					
N	L_s	β	$k = 1$	$k = 2$	$k = 3$
3	64	5.799	0.105(8)		
4	32	10.635	0.1967(89)	0.335(13)	
6	16	24.515	0.2343(87)	0.474(25)	0.657(36)
8	12	43.965	0.2835(103)	0.485(43)	0.69(10)

Table 9: The masses of the lightest time-like k -loops in the confined phase at $T = T_c$.

am_k at $a \simeq 1/5T_c$: deconfined					
N	L_s	β	$k = 1$	$k = 2$	$k = 3$
3	64	5.799	0.080(6)		
4	32	10.635	0.191(34)	0.185(32)	
6	16	24.515	0.359(14)	0.346(13)	0.346(12)
8	12	43.965	0.418(14)	0.405(13)	0.402(12)

Table 10: The lightest non-zero masses coupling to the time-like k -loop in the deconfined phase at $T = T_c$.

am_t at $a \simeq 1/5T_c$: SU(4)				
L_s	β	$C : k = 1$	$C : k = 2$	D
32	10.635	0.1967(89)	0.335(13)	0.185(32)
20	10.635	0.203(10)	0.312(20)	0.215(20)
16	10.635	0.195(20)	0.24(4)	0.25(3)
20	10.642	–	–	0.240(20)
20	10.633	0.185(10)	0.255(20)	–
16	10.630	0.204(15)	0.27(4)	–

Table 11: The lightest non-zero masses coupling to the time-like k -loop in the confined (C) and deconfined (D) phases at $T \simeq T_c$ on various volumes.

$2am_D$ for $T \geq T_c$						
N	β	$T = T_c$	$T = 5T_c/4$	$T = 5T_c/3$	$T = 5T_c/2$	$T = 5T_c/2; L_s = 6$
3	5.80	–	0.615(21)	1.040(15)	1.596(40)	–
4	10.635	–	0.660(8)	1.053(19)	1.643(40)	1.578(30)
8	44.0	0.527(11)	0.670(12)	1.054(20)	1.599(46)	1.62(5)

Table 12: The lightest non-zero mass that couples to the time-like flux loop in the deconfined phase for $a \simeq 1/5T_c$ on $L_s = 8$ lattices (unless otherwise indicated).

SU(8) : $am_s(t = an_t)$		
n_t	D	C
1	1.326(7)	1.527(11)
2	1.187(24)	1.377(40)
3	1.173(81)	1.16(15)
4	1.44(39)	1.20(42)

Table 13: Effective masses extracted at $t = an_t$ from correlators of spacelike Polyakov loops on 12^35 lattices at $T = T_c$ in the confined, C , and deconfined, D , phases.

$am_s(k)$ for $T \geq T_c$						
N	k	$T = T_c$	$T = 5T_c/4$	$T = 5T_c/3$	$T = 5T_c/2$	$T = 5T_c/2; L_s = 6$
3	1	–	0.753(7)	1.119(11)	2.027(42)	–
4	1	–	0.835(7)	1.192(12)	2.211(66)	1.607(23)
	2	–	1.126(17)	1.59(4)	2.52(32)	2.09(8)
8	1	0.695(9)	0.910(11)	1.311(19)	2.39(13)	1.805(32)
	2	1.171(26)	1.610(34)	2.12(12)	–	3.1(7)
	3	1.507(41)	1.933(81)	2.29(32)	–	–
	4	1.603(72)	2.41(23)	2.75(99)	–	–

Table 14: The spacelike k -loop masses on 8^35 lattices (unless otherwise indicated) in the deconfined phase.

interface tension				
N	σ_{cd}/T_c^3	fit range	χ^2/n_{df}	n_{df}
3	0.0200(6)	16-40	1.51	3
4	0.1208(56)	14-20	0.37	2
6	0.394(11)	8-14	6.02	2
8	0.56(10)	8-10	-	0

Table 15: The tension of the confining-deconfining interface, in units of T_c , for various $SU(N)$ gauge theories, extracted from the $V \rightarrow \infty$ extrapolations in Fig.12. All for fixed a : $aT_c = 1/5$. The best fit χ^2 and the number of degrees of freedom, n_{df} , are shown.

bulk transition			
N	lattice	β_b^\downarrow	β_b^\uparrow
5	8^4	16.6565(5)	16.6565(5)
5	10^4	16.6550(5)	16.6550(5)
5	12^4	16.6550(10)	16.6550(10)
6	4^4	24.100(25)	24.475(25)
6	6^4	24.290(5)	24.480(5)
8	4^4	43.25(5)	44.85(5)
8	6^4	43.60(5)	44.90(5)
12	4^4	98.5(1)	103.9(1)
12	8^35	98.7(1)	-

Table 16: The location of the strong-weak coupling bulk transition when decreasing or increasing β from large or small values respectively. For various $SU(N)$ groups on the lattices shown.

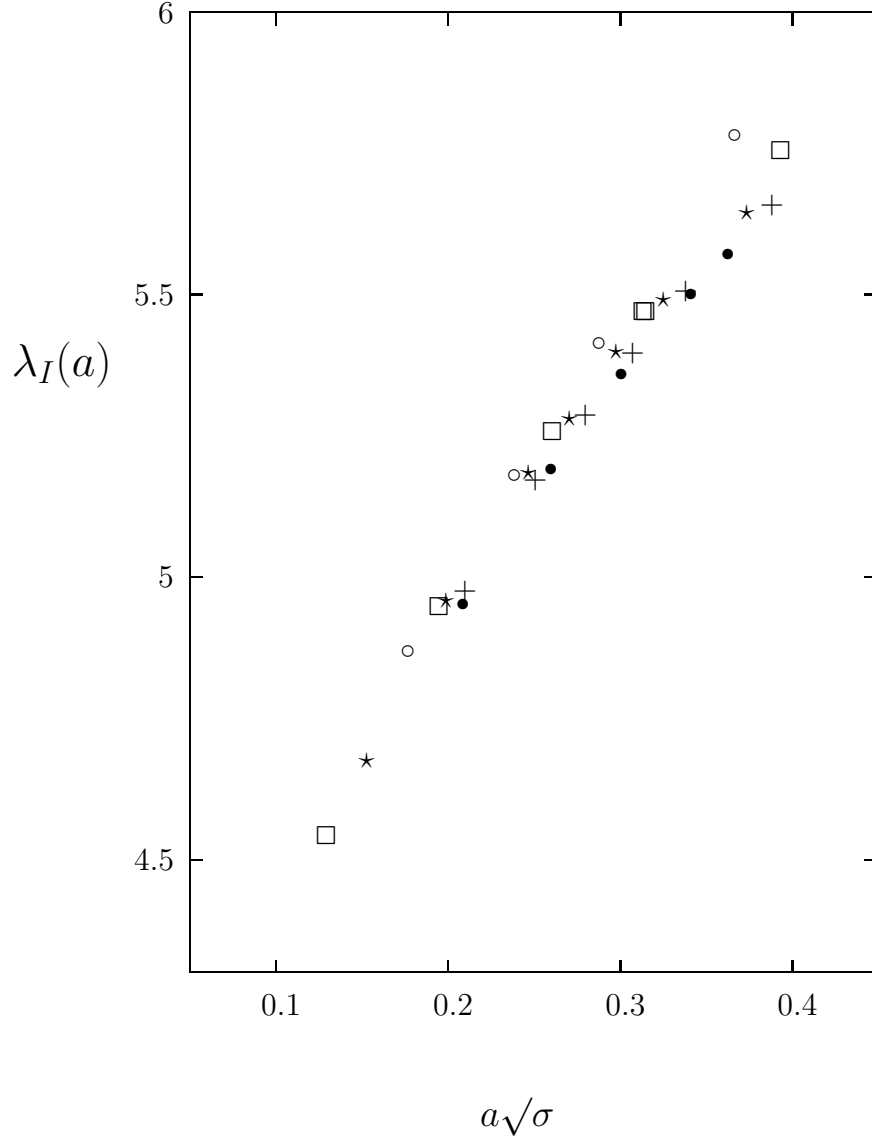


Figure 1: The value of the 't Hooft coupling on the scale a , as obtained from β in eqn(25), for $N = 2(\circ), 3(\square), 4(\star), 6(+), 8(\bullet)$, plotted against the values of a expressed in physical units.

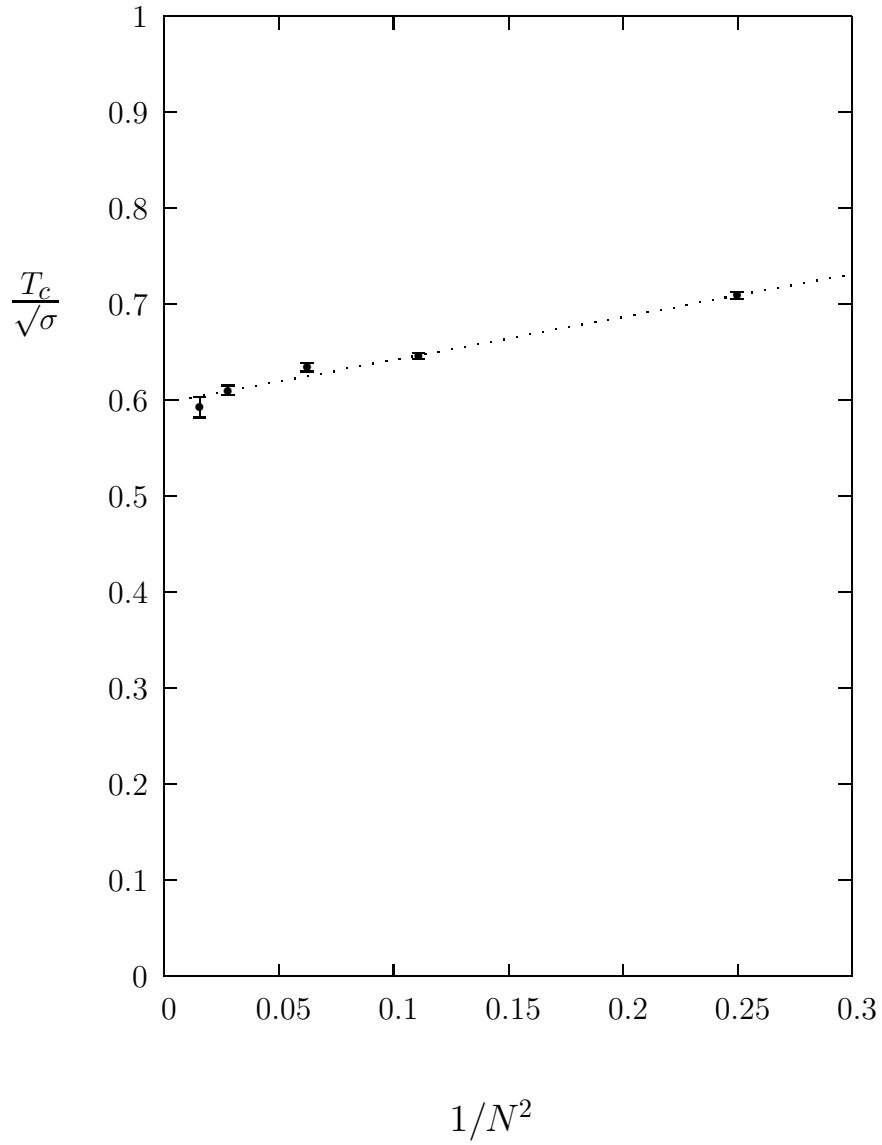


Figure 2: The $SU(N)$ continuum deconfining temperature in units of the string tension, with an extrapolation to $N = \infty$ using a leading $O(1/N^2)$ correction.

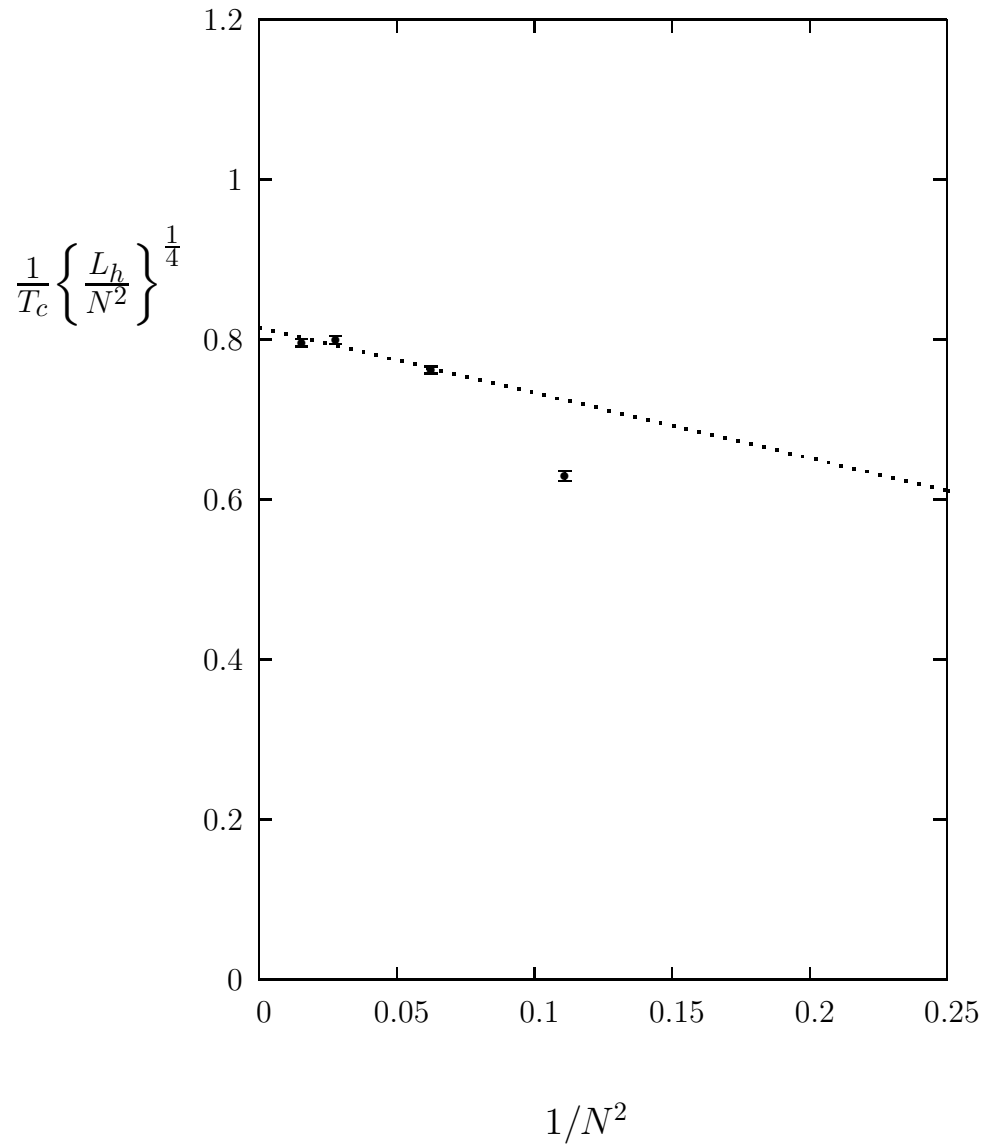


Figure 3: The latent heat calculated at $a = 1/5T_c$ for various $SU(N)$ groups.

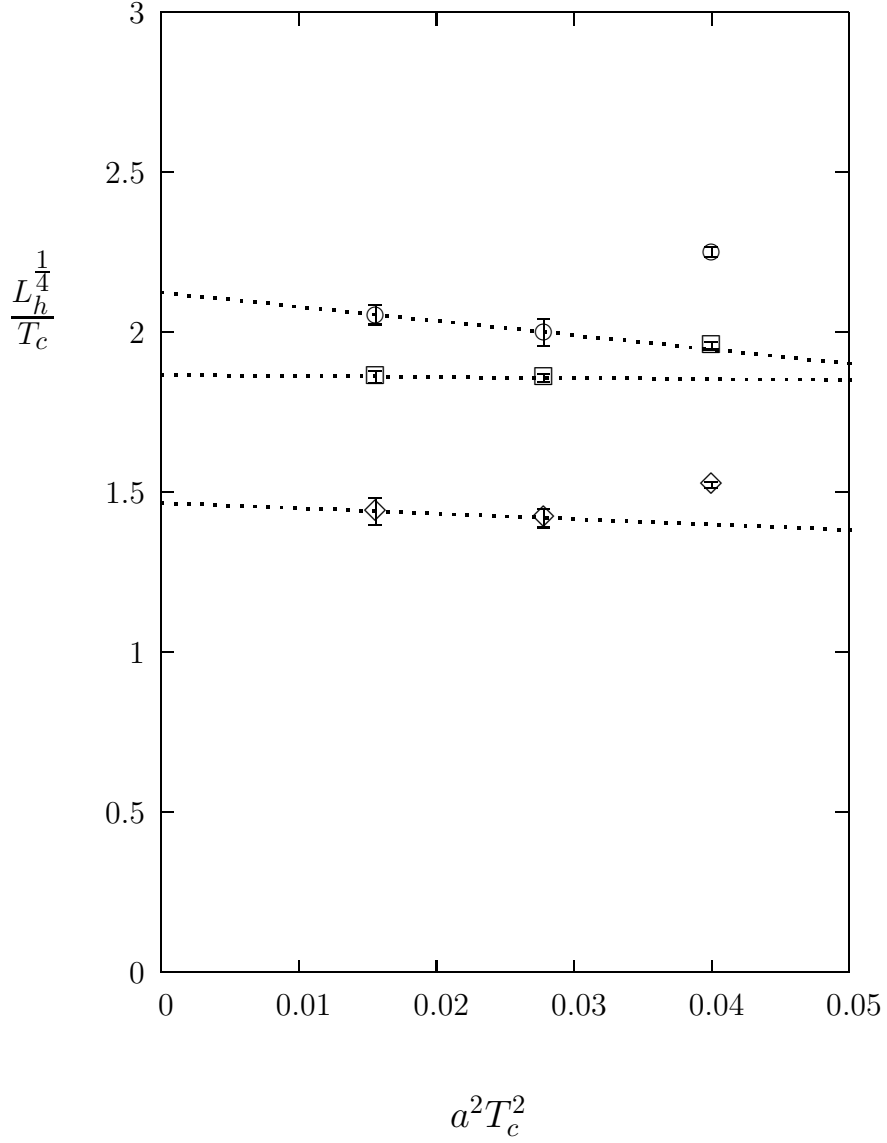


Figure 4: The deconfining latent heat in SU(4), \diamond , SU(6), \square and SU(8), \circ gauge theories at various a , with extrapolations to the continuum limit using a $O(a^2)$ correction.

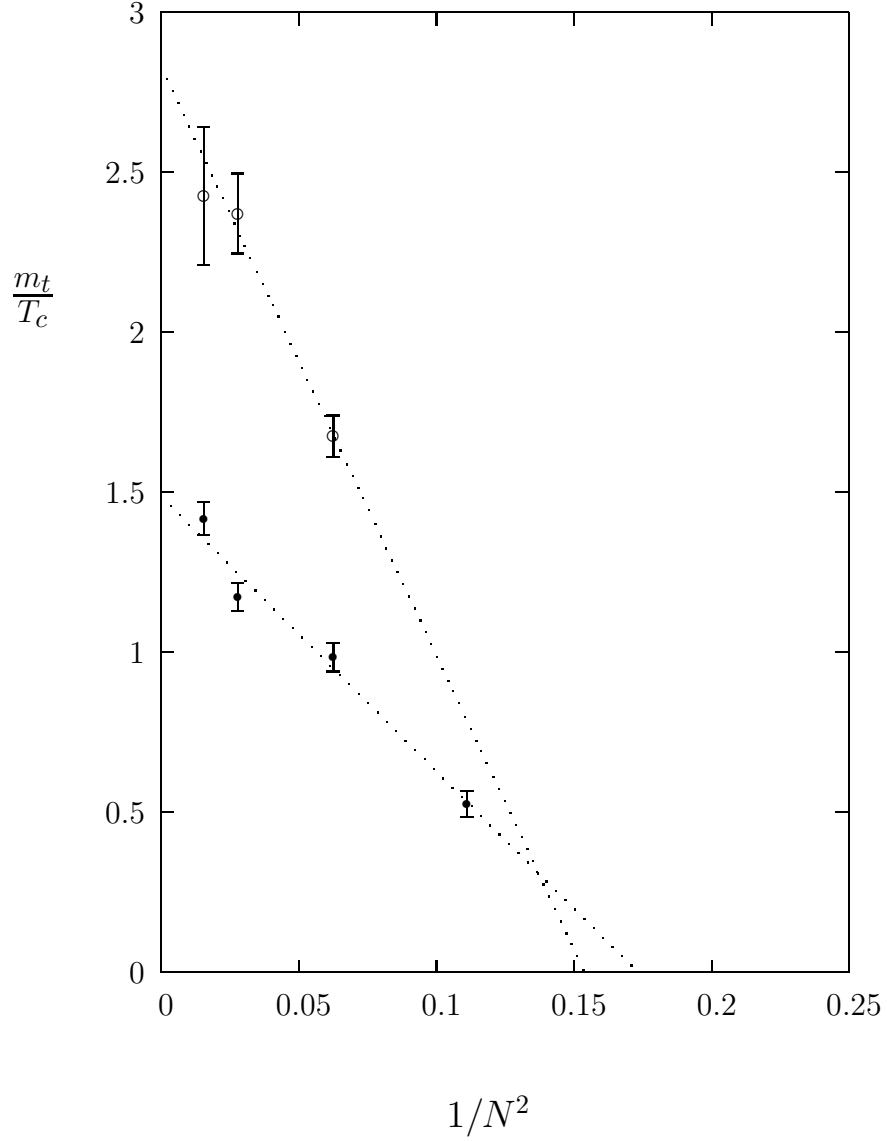


Figure 5: The masses of the lightest $k = 1$ (\bullet) and $k = 2$ (\circ) flux loops that wind around the time-torus, in the confining phase at $T = T_c$, $a = 1/5T_c$ for various $SU(N)$ gauge theories.

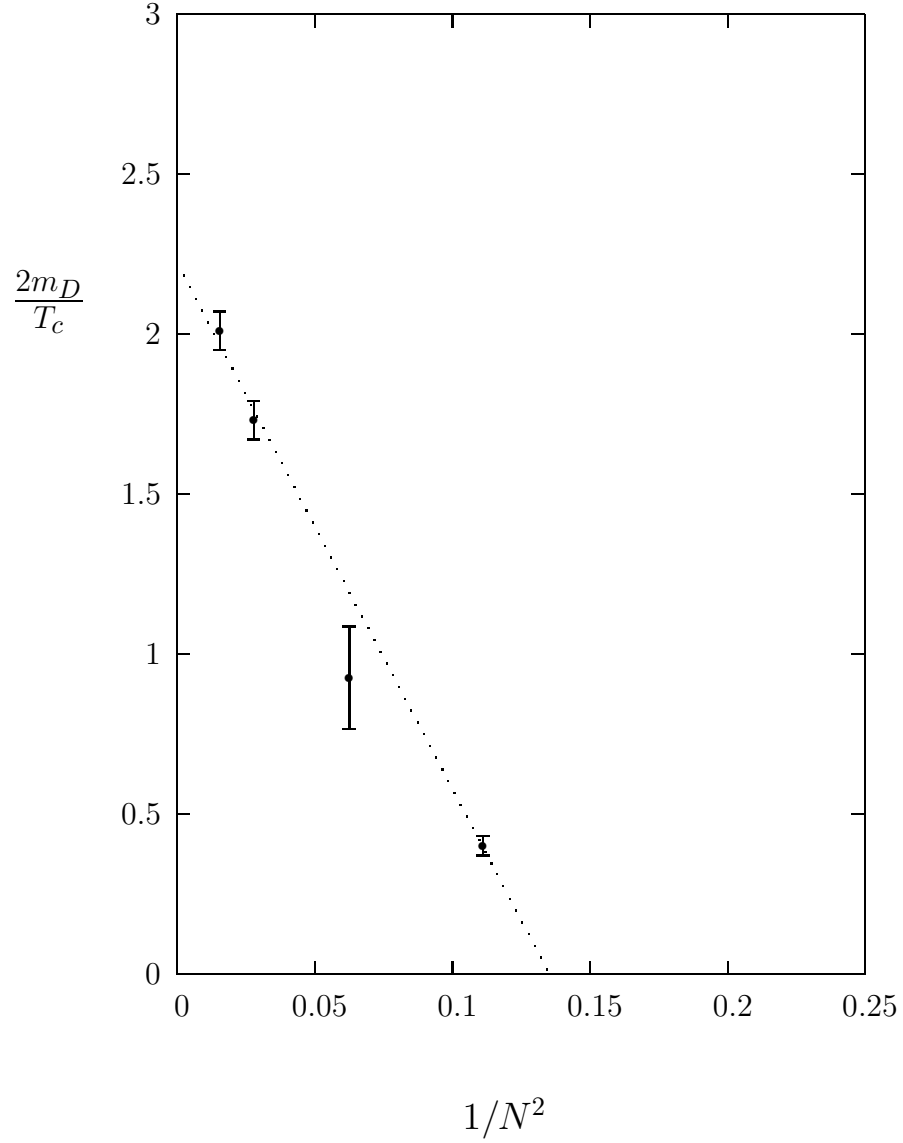


Figure 6: The lightest mass that couples to the vacuum subtracted Wilson line winding around the time-torus, in the deconfined phase at $T = T_c$ and $a = 1/5T_c$ for various $SU(N)$ gauge theories.

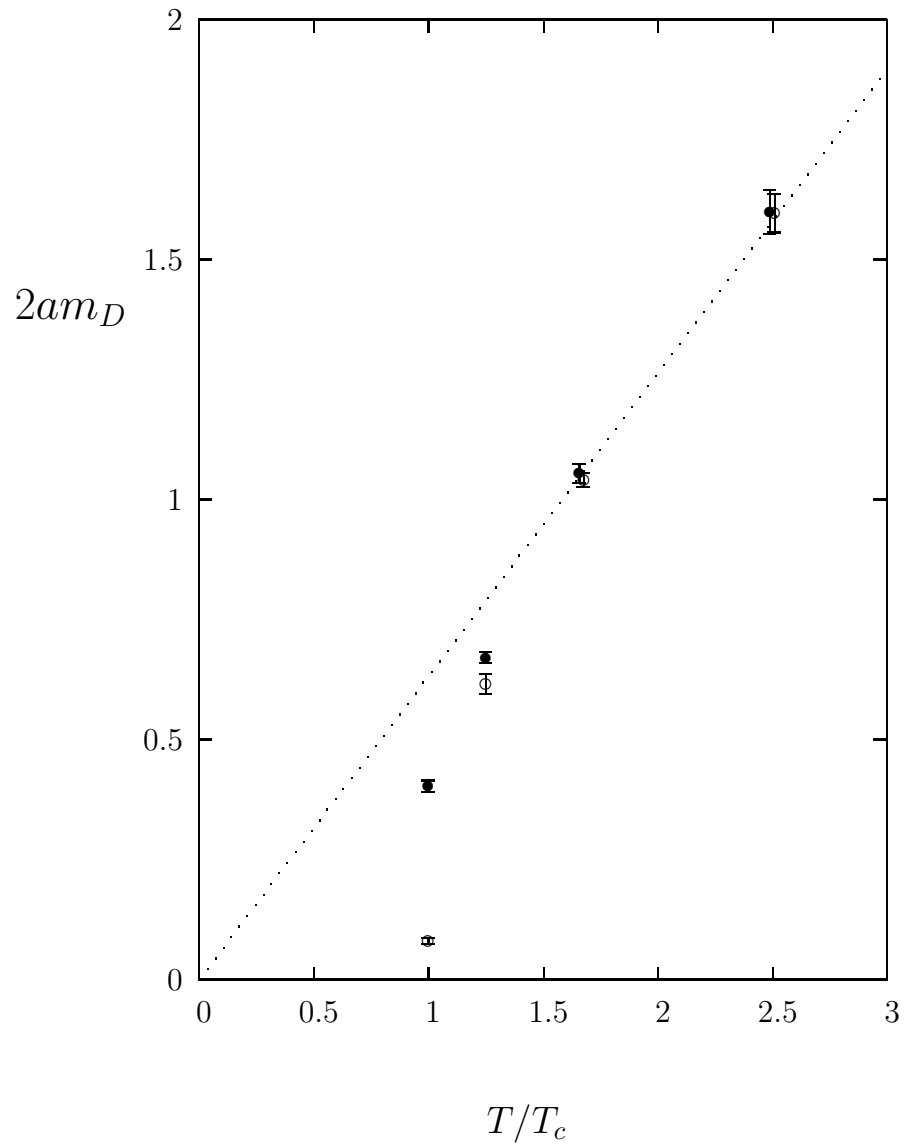


Figure 7: The electric screening mass plotted against T/T_c for SU(3) (\circ) and SU(8) (\bullet).

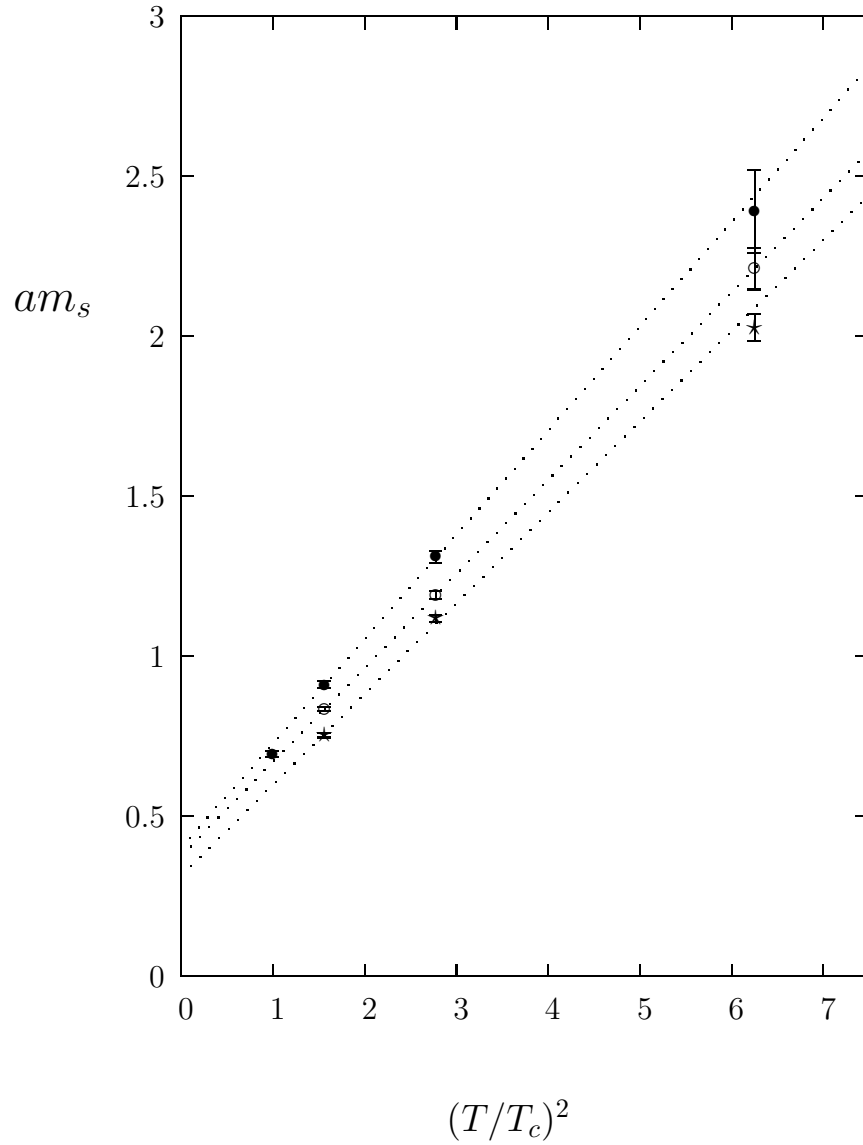


Figure 8: The mass of the lightest $k = 1$ flux loop that winds around a spatial torus. Plotted against T^2 for SU(3) (\star), SU(4) (\circ) and SU(8) (\bullet), all at $a \simeq 1/5T_c$.

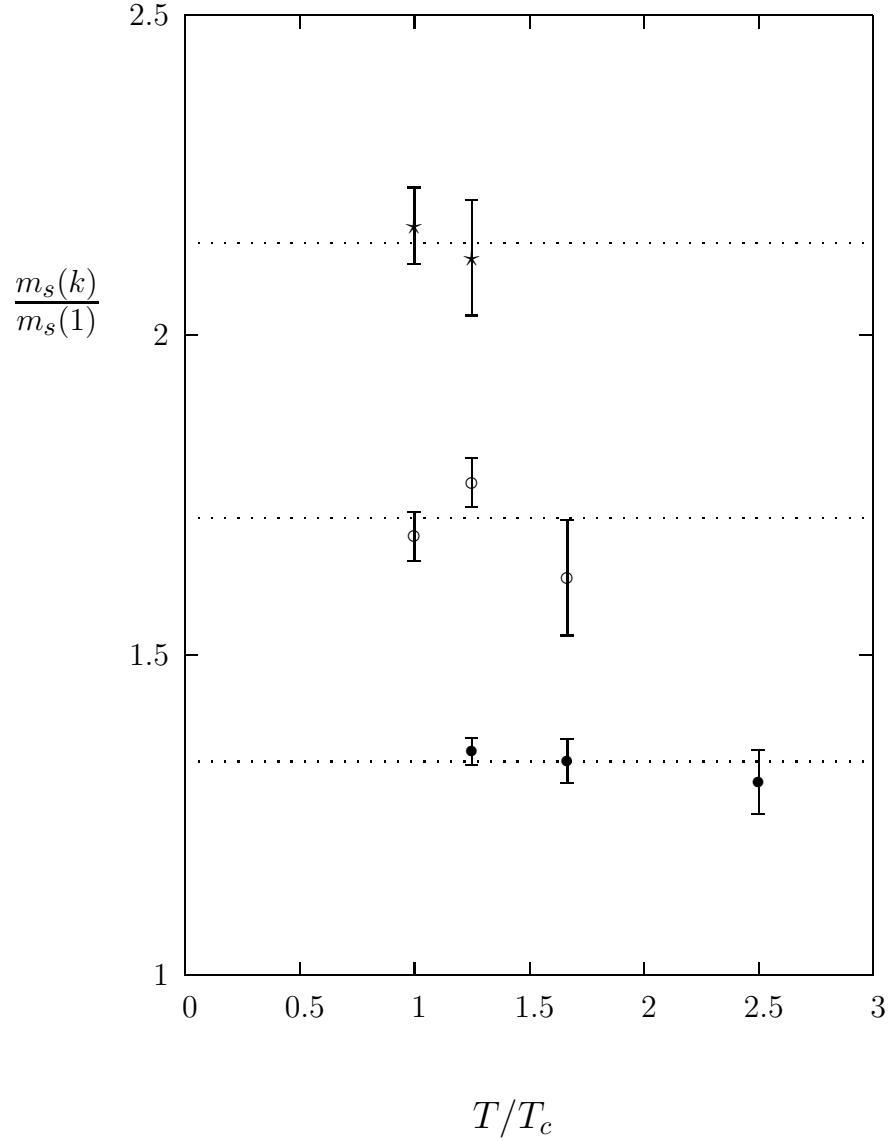


Figure 9: The mass ratio of the $k = 2$ to $k = 1$ spatial loops in SU(4) (●) and in SU(8) (○), and of the $k = 3$ to $k = 1$ loop in SU(8) (★). All in the deconfined phase and for $a \simeq 1/5T_c$. High T Casimir scaling predictions are shown for comparison.

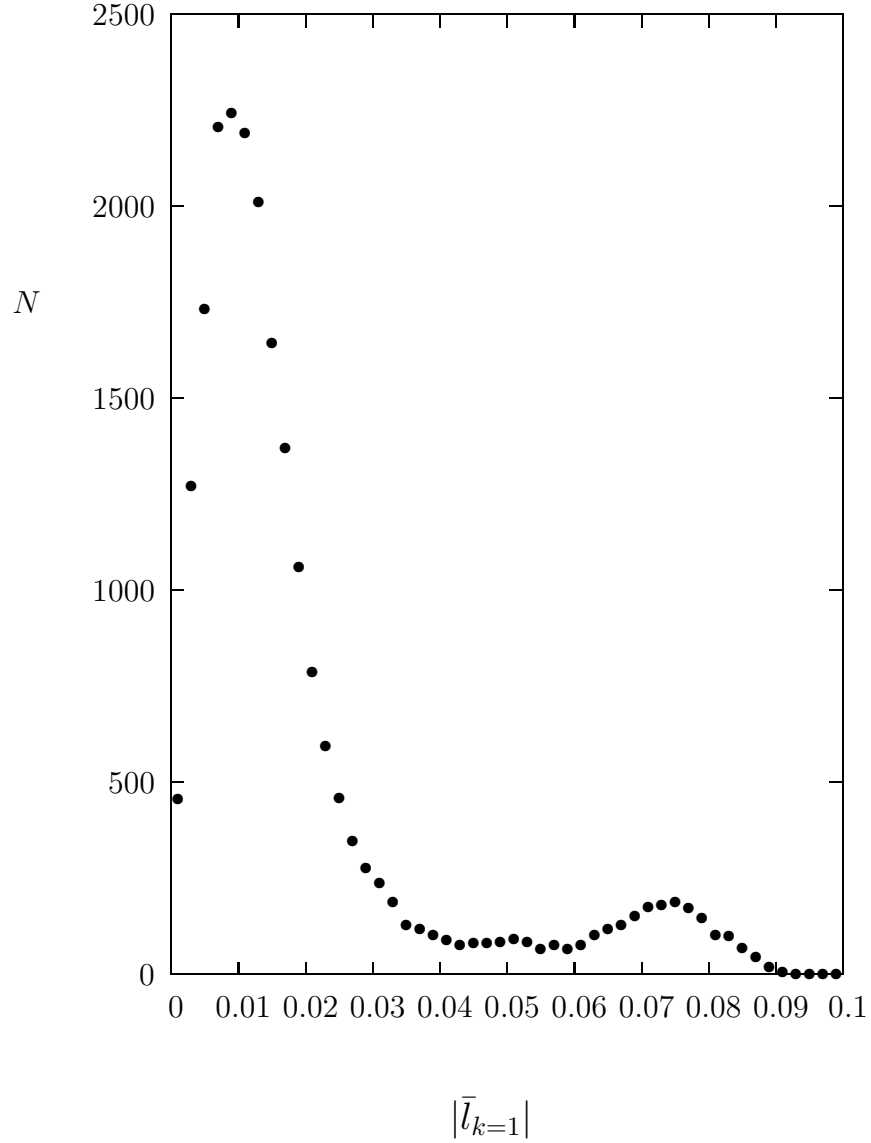


Figure 10: Histogram of timelike $k = 1$ Polyakov loops averaged over single 20^{35} lattice fields in $SU(4)$ at $T \simeq T_c$. Separate confined and deconfined peaks are visible.

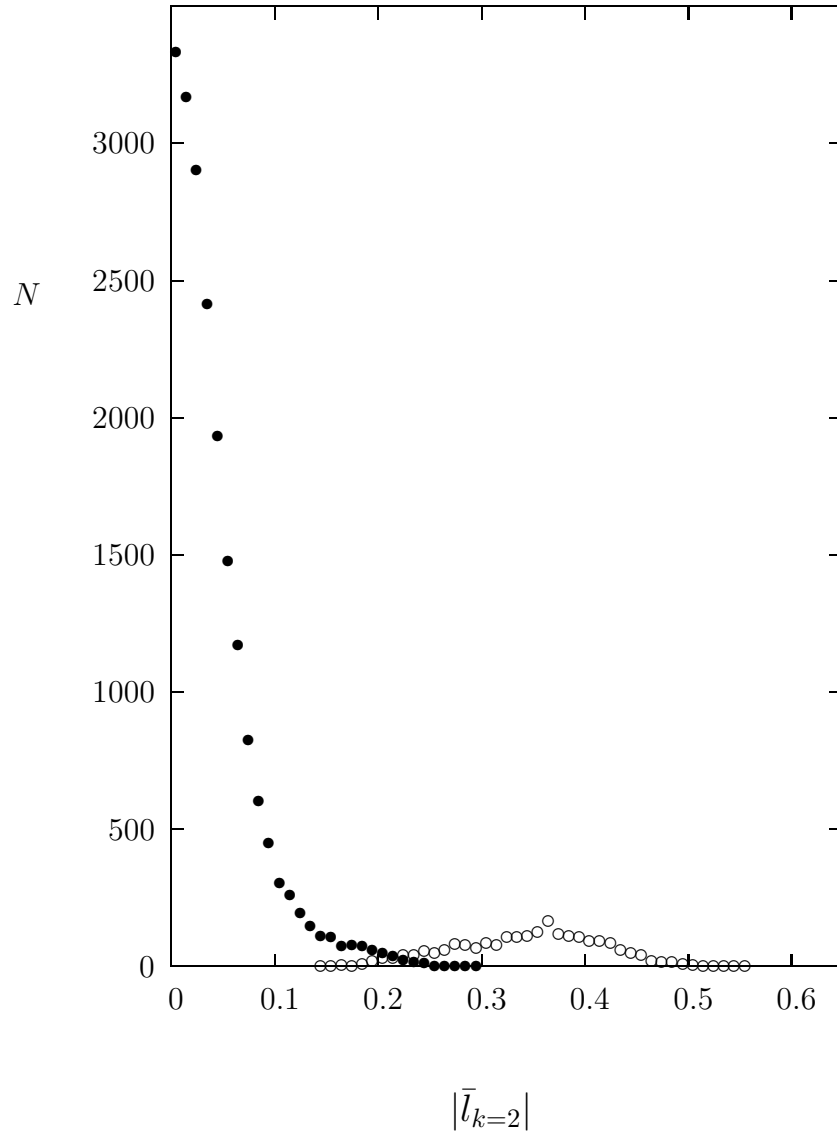


Figure 11: As in Fig.10 but for (antisymmetric) $k = 2$. From lattice fields with $|\bar{l}_{k=1}| \leq 0.05$, \bullet , and with $|\bar{l}_{k=1}| > 0.05$, \circ .

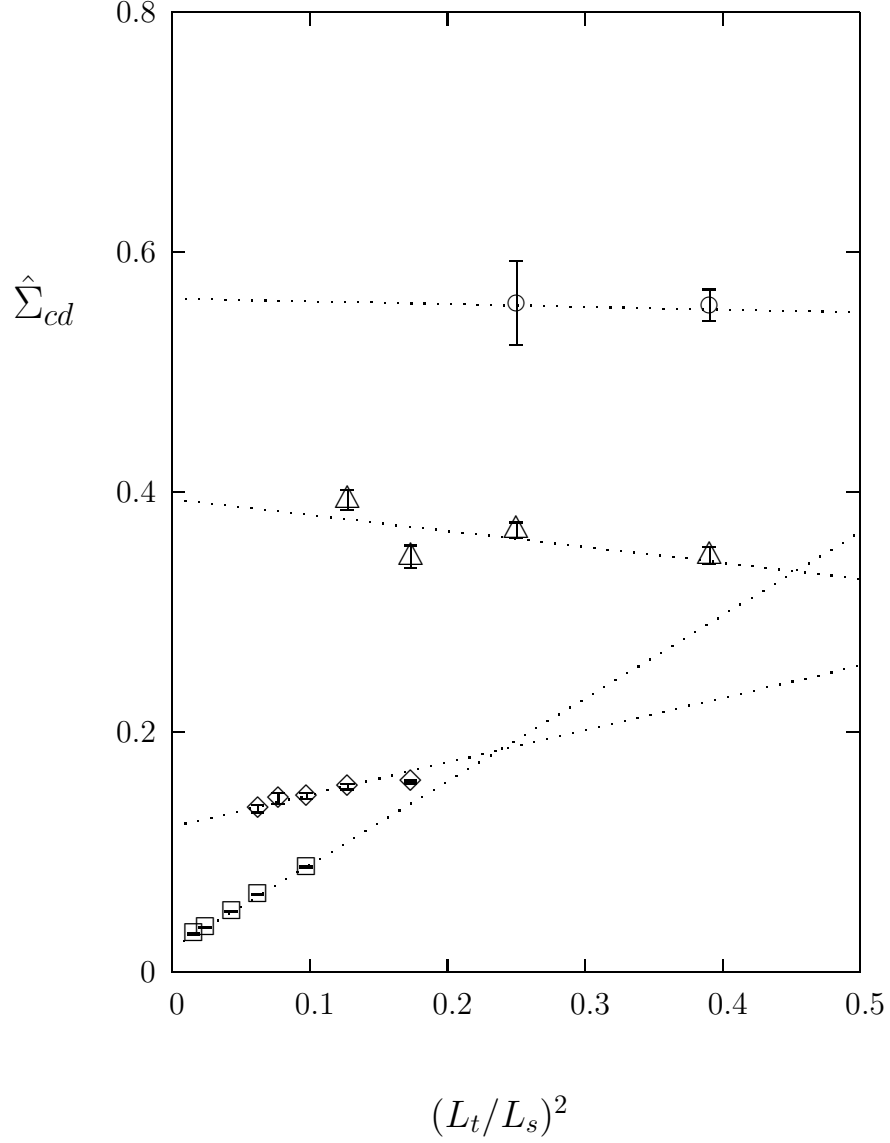


Figure 12: The quantity $\hat{\Sigma}_{cd}$ defined in eqn(50) whose $L_s = \infty$ intercept is the interface tension, σ_{cd}/T_c^3 . Calculations for SU(3), \square , SU(4), \diamond , SU(6), \triangle and SU(8), \circ . All are for $a \simeq 1/5T_c$. Linear extrapolations to infinite V are shown.

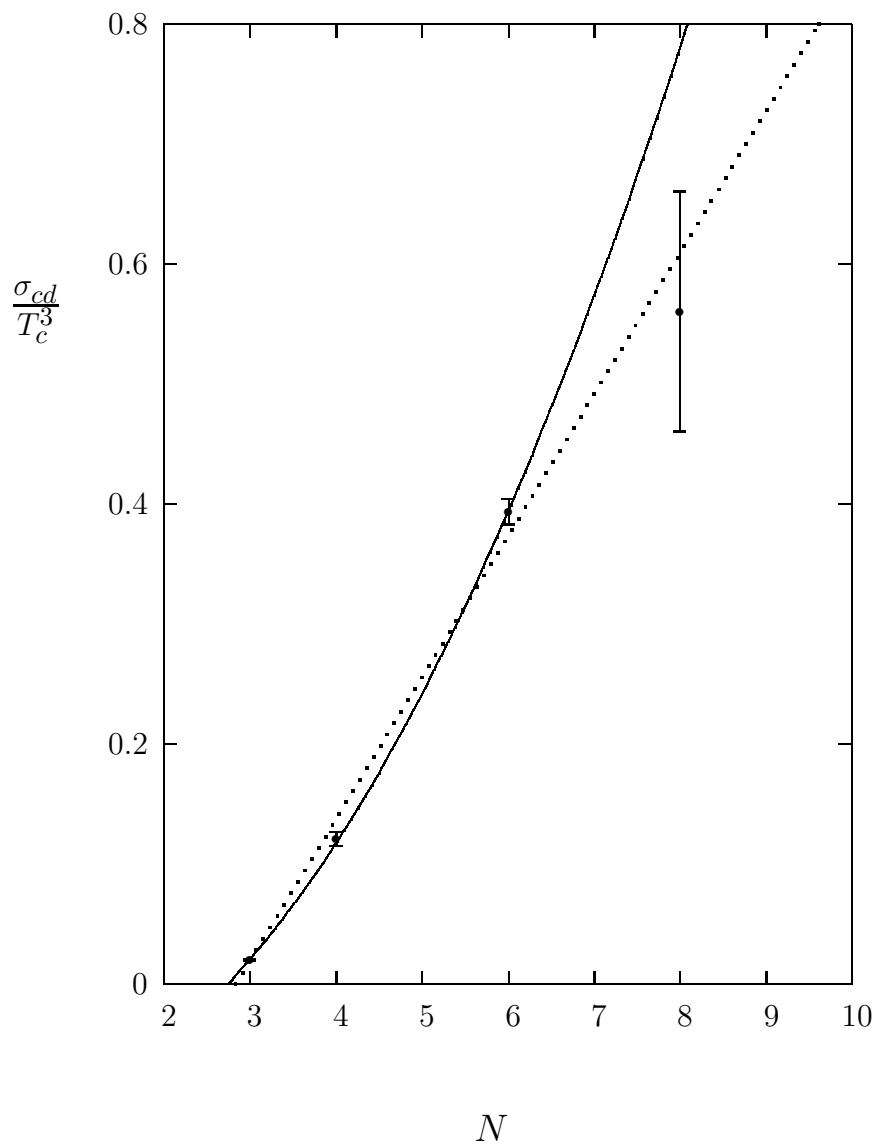


Figure 13: The interface tension at the fixed lattice spacing $a \simeq 1/5T_c$ plotted against N . Also shown are the best linear and quadratic fits.

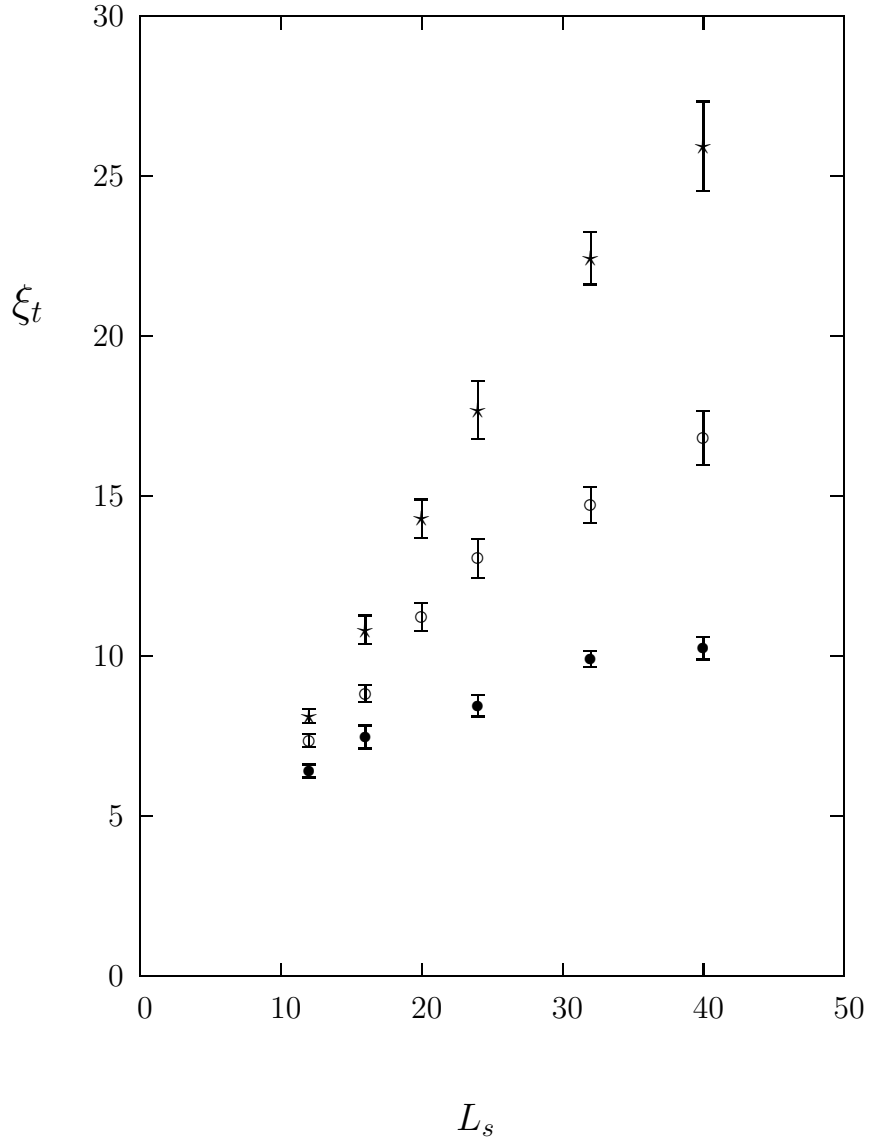


Figure 14: The correlation length near the SU(2) deconfinement transition, as a function of the spatial lattice size. For $\beta = 2.360$ (\bullet), $\beta = 2.3675$ (\circ), and $\beta = 2.3725$ (\star) on L_s^3 lattices where $\beta_c(V = \infty) = 2.3714(6)$ [2].